Numerical Study of Surface Tension Driven Convection in Thermal Magnetic Fluids

(Sumbitted to the *Journal of Crystal Growth*)

[1]Bhattacharjee, Pratik &
[2]Riahi, Daniel N.

Departments of Aerospace Engineering[1] & Theoretical and Applied Mechanics[2],
University of Illinois, Urbana Champaign
319-D[1] & 112[2] Talbot Laboratory, 104 S. Wright Street
Urbana IL 61801 , USA

Abstract

Microgravity conditions pose unique challenges for fluid handling and heat transfer applications. By controlling (curtailing or augmenting) the buoyant and thermocapillary convection, the latter being the dominant convective flow in a microgravity environment, significant advantages can be achieved in space based processing. The control of this surface tension gradient driven flow is sought using a magnetic field, and the effects of these are studied computationally. A two-fluid layer system, with the lower fluid being a non-conducting ferrofluid, is considered under the influence of a horizontal temperature gradient. To capture the deformable interface, a numerical method to solve the Navier-Sokes equations, Heat equations and Maxwell's equations was developed using a hybrid Level Set/ Volume-of-Fluid technique. The convective velocities and heat fluxes were studied under various regimes of the thermal Marangoni number Ma, the external field represented by the magnetic Bond number Bo_m, and various gravity levels, Fr. Regimes where the convection were either curtailed or augmented were identified. It was found that the surface force due to the step change in the magnetic permeability at the interface could be suitably utilized to control the instability at the interface.

Symbols

CHT,x or y: Convective heat Transfer, x and y direction
Ma: Marangoni Number
Bo,m: Magnetic Bond Number
Fr: Froude Number
Gr: Grashof Number
Re: Reynolds number
We: Weber Number
L: Length scale
u,v: velocity in the x- and y- direction

ρ: Density
Cp: Coefficient of Heat
T: Temperature
σ: constant of surface tension
B: External magnetic field
H: Magnetization
μ: Magnetic permeability
φ: Level Set function

1 Introduction

Systems of immiscible fluid layers can be found in a number of applications in areas such as materials processing and convective heat and mass transfer. In the area of materials processing we can provide examples such as use of encapsulants in float zone crystal growth process and a buffer layer in industrial Czochralski crystal growth process to prevent convection due to the surface tension gradient force. In the microgravity and space-processing realm, the exploration of other planets requires the development of enabling technologies in several fronts. The reduction in the gravity level poses unique challenges for fluid handling and heat transfer applications. By controlling (curtailing or augmenting) the buoyant and thermocapillary convection, the latter is the dominant convective flow in a microgravity environment, significant advantages can be achieved by pursuing space based processing.

The study considers thermal convective flow and its control using magnetic fluids and magnetic fields in a two immiscible fluid-layer system subjected to an imposed temperature gradient, which is assumed to be parallel to the averaged location of the interface between the two layers. Using an external magnetic field one can essentially dial in a volumetric force – gravity level, on the magnetic fluid and thereby affect the system thermo-fluid behavior.

Convection control (flow reduction or enhancement) is an important problem with many practical applications; In terrestrial applications such as heat exchanges where augmented heat transfer is desirable in order to achieve higher efficiencies, gravity induced convection due to thermal buoyancy force assists fluid flow and heat transfer. In reduced-gravity situations heat transfer enhancement is important and is solely achieved using forced flow configurations; In semiconductor crystal growth applications, however, convection can cause undesirable motions in the melt resulting in higher defect densities, improper mixing resulting in reduced inhomogeneity (dopant distribution) and therefore non uniform properties (electrical) of the grown crystals. Experiments conducted in space have yielded promising results for alloy-semiconductors that are traditionally difficult to grown on Earth because of wide disparities in the material properties (densities) of the components; (iv) In containerless processing of materials that is used to significantly reduce the thermal and contact stresses and impurity incorporation in the grown crystal, significant flows due to Marangoni (thermocapillary) and solutocapillary convection plaque the growth process and the resulting crystal quality. Again different methods of convection control such as liquid encapsulation, static and dynamic magnetic field approaches have been used to reduce the so-called convective contamination in the system. The encapsulant also serves to reduce the evaporation of a volatile component in the crystal growth, for example, Boron oxide encapsulant is used in GaAs crystal growth to reduce the volatile As from escaping the system and thereby affecting the crystal stoichiometry.

While a level of convection control can be realized by using magnetic means, usually through Lorentz dissipation, the force reduces as the system flow reduces so that in order to approach diffusion limited conditions (Pe < 1, where Pe is the Peclet number, a ratio of the system thermal to viscous transport), large magnetic fields (~1 Tesla) are required. Dynamic magnetic fields such as rotating magnetic fields (rmf) and traveling magnetic fields (tmf) are also being studied for this purpose. It has been shown that significantly reduced magnetic field strengths (~3 orders of magnitude smaller) are required for rmf damping than a static one. Magnetic damping is non-intrusive and its intensity can be controlled externally. A few studies are ongoing that utilize a magnetic field gradient and the variation of the material susceptibility with temperature to control fluid flow in a system. In this approach, the magnetic field-field gradient product acts as a body force similar to gravity and can be tailored to either curtail or enhance the fluid flow. This can be likened to prescribing a desired gravity-level on the system and is a powerful experimental tool for simulating variable and reduced gravity environments.

The main objectives of the study are briefly as follows. For pure buoyancy driven flow studies, we will utilize a working fluid that is magnetically responsive (ferrofluid). For working fluids that are not magnetically responsive (weak diamagnetic properties) we propose the use of an additional fluid, such as a ferrofluid, to form an immiscible double-layer system configuration. For the latter, we would like to determine the flow solutions in both layers for deformed interface cases. We would like to carry out stability analysis to determine the range of the parameter values under which steady and time dependent solutions are stable and thus preferred. We want to determine conditions under which such solutions are most realistic and search for the conditions on the magnetic fields and fluids where convection is maximally reduced (halt condition). For the deformed interface cases, we would like to examine the interface dynamics and the roles played by the magnetic fields with different strength and orientation on the flow intensity, flow patterns, convective instability, surface tension, due to interface and free surface, and fluid viscosity.

1.1 Immiscible Fluid Layers

There have been a number of studies on the effects of convection in systems of immiscible fluid layers subjected to imposed temperature gradients (Szekely and Todd 1971; Simanovskii 1979; Bourde and Simonovskii 1979; Knight and Palmer 1983; Kimura *et al.*1985; Sparrow *et al.*1986; Myrum *et al.*1986; Nepomnyashchy and Simanovskii1990; Simonovskii *et al.*1992; Liu and Roux 1992; Georis *et al.* 1993; Ramachandran 1993; Doi and Koster 1993; Prakash and Koster 1993, 1994a, 1994b, 1994c; Georis *et al.*1994; Georis and Legros 1995; Kats-Demianets *et al.*1997a,b; Georis *et al.*1997; Nepomnyashchy and Simanovskii1997; Kliakhandler *et al.*1998; Xu and Zebib1998; Nepomnyashchy and Simanovskii 1999; Georis *et al.*1999; Kliakhandler and Nepomnyashchy 1999; Hamed and Florian 2000; Monti2001; Velarde and Nepomnyashchy 2001; Smith *et al.* 2002). Ramachandran (1993) investigated numerically the effects of buoyancy and surface tension gradient forces on thermal convection in a system with two horizontal immiscible fluids subjected to an imposed lateral temperature gradient. The investigated flow system consisted of a lighter fluid layer on top of a heavier fluid layer, and both layers were contained in a two-dimensional open cavity. Both upper free surface and the interface between the two fluid layers were assumed to be flat and undeformable in his calculations. Ramachandran (1993) solved the governing system of equations and boundary conditions by using a control volume-based finite difference scheme for two cases of immiscible fluids. The main results were that steady-state calculations predicted dramatically different flows when interfacial tension effects were included, and complex flow patterns, with induced secondary flows, were found in both of the fluid layers. Doi and Koster (1993) investigated analytically and numerically two-dimensional pure thermocapillary convection in two immiscible fluid layers with an upper free surface. Both the free surface and the interface were assumed to be horizontal flat with zero deformation. Their results are briefly as follows. First, based on some approximations, they found an analytical solution in the steady state for infinite horizontal extent of the layers. Under a zero gravity environment, four different flow profiles exist which are controlled by a parameter, λ. This parameter is ratio of the temperature rate of change of the interfacial tension between the two layers to the temperature rate of change of the surface tension of the upper layer. They found three 'halt conditions' which stop the flow motion in the lower layer. They identified the technologically relevant halt condition as $\lambda = 0.5$. Next, they studied numerically the effects of the vertical end walls on the flow. They determined conditions on the flow parameters under which the above halt condition can be valid, and they showed that for $0 < \lambda < 0.2$, thermocapillary convection can greatly be suppressed in the encapsulated liquid layer at some higher Marangoni number. A direct numerical simulation of thermal convection in an enclosed cavity filled by three immiscible fluid layers and subjected to an imposed temerature gradient parallel to the interfaces were carried out by Georis *et al.*(1997), where the deformations of the interfaces were neglected. These authors found, in particular, an essential influence of the nonlinear effects for particular range of the parameters, such as Rayleigh and Marangoni numbers, and that depending on the value of the Rayleigh number, the flow intensity was observed in different layers

In regard to the investigated cases of convective flows in systems with deformed interface and/or deformed free surface, kinematic and dynamic conditions need to be satisfied on the deformed surfaces (Davis 1987), which were treated either by applying some approximations or by numerical means (Sen and Davis 1982; Smith 1986; Hjellming and Walker 1987; Riahi and Walker1989; Lie, Riahi & Walker 1989; Hamed & Florian 2000). Sen and Davis (1982) studied steady thermocapillary flows in two-dimensional slot with an imposed temperature gradient along the free surface. They used an asymptotic theory in the limit of small aspect ratio A of the slot to determine the fluid and thermal field and the interfacial shapes and found that deformation of an interface between the liquid flow in the slot and the ambient passive gas was small of order A. Hjellming and Walker (1987) investigated analytically the melt motion due to buoyancy and thermocapillarity in a Czochralski crystal puller with an axial magnetic field. They found, in particular, that thermocapillarity, which becomes progressively more dominant as the crystal grows and the melt depth decreases, is sensitive to changes in the amount of heat lost through the part of the deformed free surface adjacent to the crystal. Riahi and Walker (1989) investigated the deformed free surface stability and shape of the melt during the float zone crystal growth process with the presence of the electromagnetic body force due to a radio-frequency induction coil. They found that this force pinches the float zone and produces a smaller minimum radius, relative to the feed rod and crystal radii, and for coil, which is close to the free surface, a sufficiently strong electromagnetic force destabilizes the free surface of the zone. Lie, Riahi and Walker (1989) investigated buoyancy driven flow, which was due to the temperature gradient in the melt of a float zone, and the surface tension driven flow, which was due to the non-uniform temperature distribution along the deformed free surface of the zone, in the presence of a strong axial magnetic field. The non-cylindrical deformed shape of the free surface of the zone was found to have a profound effect on the melt motion. Their results indicated that the regions near the free surface were controlled mainly by the thermocapillarity, while the inner region was dominated by the buoyancy driven flow. Hamed and Florian (2000) investigated computationally two-dimensional Marangoni convection in a cavity with differentially heated sidewalls. Their study took into account the complete effects of the deformed interface between the liquid layer and a passive gas. They found that under certain parameter regime, multiple states with steady and oscillatory flows were possible and transition between the steady and the oscillatory states appeared to involve a nonlinear instability process.

1.2 Hele-Shaw cell systems

There have been a number of studies of flow of two immiscible fluids in a Hele-Shaw cell (Saffman and Taylor 1958; Zeybek and Yortsos 1991; McCloud and Maher 1995; Gondret and Rabaud 1997; Miranda and Widom 2000), which provides a simple mathematical and experimental model for theoretical and experimental studies of the two-layer systems in order to hopefully gain further physical understanding of the qualitative aspects of related but more complex flow pattern-evolution problems. Most of the studies of the two-layer flow in the Hele-Shaw cell have been focused on viscous fingering that was first studied by Saffman and Taylor (1958) who considered two immiscible viscous fluids moving in the narrow space between two parallel plates of a Hele-Shaw cell. They demonstrated that air driven into glycerin in such a cell could form a steady pattern in the form of a single finger of air, and the flow equations admit a family of solutions one of which agrees well with the experimental observation. McCloud and Maher (1995) reviewed experimental perturbations to Saffman-Taylor (S-T) flow problem, which provides a simple case of nonlinear interfacial pattern formation. In a number of experiments perturbations have been added to the S-T problem in order to learn more about interface dynamics and about the roles played by the material properties on the dynamical evolution of the resulting flow patterns. Zeybek and Yortsos (1991) studied theoretically and experimentally the long waves in parallel flow in Hele-Shaw cells. To study interface dynamics, they first derived the linear dispersion relation using normal mode approach (Drazin and Reid 1981) and then determined the solutions. Next, they used asymptotic analysis to determine the nonlinear evolution of small amplitude and long wave disturbances. They found that such disturbances are governed by Kortweg-de-Vries and Airy equations (Whitham 1974; Drazin and Reid 1981). For a symmetric case, experimental evidence supported the theory, including the propagation of solitary waves (Whithan1974). Gondret and Rabaud (1997) studied experimentally the parallel flow in a Hele-Shaw cell of two immiscible fluids, a gas and a liquid layer, driven by an imposed pressure gradient. They observed that the interface destabilized above a critical value of the gas flow at which waves grew and propagated along the cell. Their theoretical prediction based on a linear stability analysis agreed with their experimental results.

1.3 Flow Instability

We already referred to a number of investigations for the deformed interface or deformed free surface effects on the convective flow, which involved flow instabilities under certain conditions. Here some other notable studies in the past that involved flow instabilities are briefly described. Smith and Davis (1983a) investigated instabilities in thermocapillary liquid layers by considering a horizontal liquid layer subjected to an imposed temperature gradient along the layer, which led to the flow motion due to thermocapillarity. They carried out linear stability analysis of disturbances superimposed on their detected basic flow solutions and found, in particular, that the dynamic state of the flow is then susceptible to two types of thermal-convective instabilities of either stationary longitudinal rolls, which involve the classical Marangoni instability (Pearson 1958), or unsteady hydrothermal waves, which derive their energy from the horizontal temperature gradient. In the second part of this study (Smith and Davis 1983b) the authors found, in a particular, that for a particular linearized case, the thermal field decoupled from the hydrodynamic field and the instability of the basic flow set up by the thermocapillarity is a purely isothermal one. Xu and Zebib (1998) investigated numerically oscillatory two- and three-dimensional thermocapillary convective flows in a rectangular cavity and in a box, respectively, and determined, in particular, the character and stability of such flows. For two-dimensional cases, they used a finite-volume based scheme to determine the solutions, while in three-dimensional cases a finite-volume-based primitive variable solver was used. Kliakhandler and Nepmnyashchy (1999) investigated theoretically and numerically instabilities of thermocapillary flow in three-layer systems. They derived linear and weakly nonlinear equations for the evolution of the interface and carried out linear stability analysis. They found, in particular, new types of long-wavelength instabilities, which persisted at arbitrary small Reynolds number. Hoyas *et al.* (2002) investigated thermo-convective instabilities in a fluid within a cylindrical annulus heated laterally. They considered a particular domain in the parameter space where buoyancy force dominated over the surface tension gradient force. They found a nonlinear basic flow computationally and carried out a linear stability calculation of the base flow. They found, in particular, that there existed stationary bifurcations to radial rolls and oscillatory bifurcations to hydrothermal waves.

1.4 Effects of magnetic fields and fluids

There have been a number of studies on the application of the effect of a magnetic field on the flow in a liquid layer (Hjellming and Walker 1987; Riahi and Walker 1989; Lie, Riahi and Walker 1989; Lie, Walker and Riahi 1990; Morthland and Walker 1996, 1997a, 1997b) or in a ferrofluid layer (Miranda and Widom 2000; Zahn 2001; Leslie and Ramachandran 2001). Applications of a strong magnetic field on flow of melt in Czochralski or float zone crystal growth processes (Hjellming and Walker 1996; Lie, Riahi and Walker 1989; Lie, Walker and Riahi 1989, 1991) led to significantly reduced effects of the inertial terms in the momentum equation and consequently the fluid flow was significantly weakened. Miranda and Widom (2000) carried out a linear stability analysis for parallel flow in a Hele-Shaw cell when one fluid was ferrofluid and a magnetic field was applied. They found that the magnetic field may provide a new mechanism for destabilizing the interface in the absence of the inertial effects. They determined the magnetic correction to the dispersion relation and suggested that parallel flow of ferrofluids can be a novel system for investigating soliton interactions. Leslie and Ramachandran (2001) pointed out the importance of establishing a solute concentration gradient in a magnetic field under microgravity conditions. In particular, an appropriate magnetic field gradient acting on the ferrofluid flow can counteract the effect of Earth's gravity effectively producing suitable low gravity conditions in an experimental laboratory. Ramachandran and

Leslie (2001) investigated numerically magnetic susceptibility effects and Lorentz force damping in diamagnetic fluids. They found, in particular, that convection damping of 50% observed in the experiment can be attributed to Lorentz force damping effects and higher level of flow reduction was possible by exploiting the fluid diamagnetic susceptibility variations.

1.5 Moving interface capturing

In dealing with moving surfaces a variety of computational methods have been developed, which can be classified basically into two categories: moving-grid and fixed-grid methods. The moving-grid method is a Lagrange-type method for treating the free surface as the boundary of a moving surface-fitted grid (Floryan and Rasmussen 1989). However, when the grids are highly distorted because of strongly deformed free surface, then rezoning or re-meshing becomes necessary, which could lead to excessive numerical diffusion if frequent rezoning is done. An important fixed-grid type method, which is based on the surface capturing approach is the so-called Level set method (LSM) (Osher and Sethian 1988), which has been used in a number of problems in applications including those in solidification and crystal growth areas (Kim *et al.* 2000; Smereka 2000). In this method one defines a function $\phi(x, y, z, t)$, called level set, with some degree of smoothness (Yue *et al.* 2003) that represents the interface at $\phi = 0$. The level sets are advected by the local velocity field. The interface can be captured at any time by locating the zero level set, which alleviates the burden of increasing grid resolution at the interface in many other numerical methods. The LSM provides convenient features for handling topological merging, breaking and self-intersecting of interfaces, and information about the interface, such as orientation and curvature can be conveniently obtained as well, so that surface tension can be accurately estimated (Yue *et al.* 2003). In addition, using LSM, extension from two to three dimensions can be done easily.

2 Equations of motion of the magnetic fluid

The Governing Equations consisting of conservation of mass, x-momentum, y-momentum and heat solved are presented below in the non-conservative form.

Continuity : $$\frac{\partial u}{\partial x}+\frac{\partial v}{\partial y}=0 \tag{2.1}$$

x - Momentum : $$\rho\frac{\partial u}{\partial t}+\rho u\frac{\partial u}{\partial x}+\rho v\frac{\partial u}{\partial y}=-\frac{\partial p}{\partial x}+\frac{\partial}{\partial x}\left(\eta\frac{\partial u}{\partial x}\right)+\frac{\partial}{\partial y}\left(\eta\frac{\partial u}{\partial y}\right)+f_m{}^x+f_{surf}{}^x \tag{2.2}$$

y - Momentum : $$\rho\frac{\partial v}{\partial t}+\rho u\frac{\partial v}{\partial x}+\rho v\frac{\partial v}{\partial y}=-\frac{\partial p}{\partial y}+\frac{\partial}{\partial x}\left(\eta\frac{\partial v}{\partial x}\right)+\frac{\partial}{\partial y}\left(\eta\frac{\partial v}{\partial y}\right)+f_m{}^y+f_{surf}{}^y+f^g \tag{2.3}$$

Heat : $$\frac{\partial\rho C_pT}{\partial t}+u\frac{\partial\rho C_pT}{\partial x}+v\frac{\partial\rho C_pT}{\partial y}=\frac{\partial}{\partial x}\left(\kappa\frac{\partial T}{\partial x}\right)+\frac{\partial}{\partial y}\left(\kappa\frac{\partial T}{\partial y}\right) \tag{2.4}$$

Maxwell's Eq.1 : $$\frac{\partial B}{\partial t}=rot[v\times B]-\frac{1}{\omega}rot[rotH] \tag{2.5}$$

Maxwell's Eq.2 : $$divB=0 \tag{2.6}$$

Maxwell's Eq.3 : $$rotH=j \tag{2.7}$$

Maxwell's Eq.4 : $$j=\omega[E+v\times B] \tag{2.8}$$

These basic equations will be expanded to a form which is suitable for discretization.

2.1.1 Magnetic body force

The magnetic body force per unit volume can be written as per Rosensweig (1985) as:

$$f_m=-\nabla\left[\mu_0\int_0^H\left(\frac{\partial M\vartheta}{\partial\vartheta}\right)_{H,T}dH\right]+\mu_0M\nabla H \tag{2.9}$$

This contains many pressure-like variables which are obtained by expanding as follows:

$$f_m=-\nabla\left[\mu_0\int_0^H M\,dH+\mu_0\int_0^H\vartheta\left(\frac{\partial M}{\partial\vartheta}\right)_{H,T}dH\right]+\mu_0M\nabla H\text{ , or} \tag{2.10}$$

$$f_m=-\nabla p_m-\nabla p_s+\mu_0M\nabla H\text{ , where}$$

$$p_m=\mu_0\int_0^H M\,dH\text{, the fluid - magnetic pressure}$$

$$p_s=\mu_0\int_0^H\vartheta\left(\frac{\partial M}{\partial\vartheta}\right)_{H,T}dH\text{, the magnetostrictive pressure} \tag{2.11-12}$$

The fluid-magnetic force term

Generally considering that $M=M(\mu,H,T)$, then

$$-\nabla p_m = -\mu_0 \nabla \int_0^H M dH = \underbrace{-\mu_0 \int_0^H \frac{\partial M}{\partial T} \nabla T dH}_{I1} \underbrace{- \mu_0 \int_0^H \frac{\partial M}{\partial \mu} \nabla \mu dH}_{I2} - \mu_0 M \nabla H \tag{2.13}$$

Considering each term separately,

Term *I1*: Although in the study, the flow is non-isothermal (i.e. $\nabla T \neq 0$), we have $\frac{\partial M}{\partial T} = 0$ as the operating conditions are within the Curie temperature limit (i.e. the temperature beyond which $\frac{\partial M}{\partial T} \neq 0$). Thus this term drops off.

Term *I2*: Linearly magnetizable fluids are considered in this study, therefore the Magnetization is written as:

$$M = \frac{(\mu - \mu_0)}{\mu_0} H \tag{2.14}$$

the term becomes:

$$-\mu_0 \int_0^H \frac{1}{\mu_0} H \nabla \mu dH = -\nabla \mu \int_0^H H dH = -\nabla \mu \frac{H^2}{2} \tag{2.15}$$

Therefore the fluid-magnetic force per unit volume:

$$-\nabla p_m = -\nabla \mu \frac{H^2}{2} - \mu_0 M \nabla H \tag{2.16}$$

The magentostrictive force term

Substituting (2.14) into (2.12)

$-\nabla p_s = -\nabla \int_0^H \vartheta \left(\frac{\partial (\mu - \mu_0) H}{\partial \vartheta} \right)_{H,T} dH$. Substituting $\rho = 1/\vartheta$

$$-\nabla p_s = \nabla \left[\int_0^H \rho \left(\frac{\partial \mu}{\partial \rho} \right)_T H dH \right] = \nabla \left[\rho \left(\frac{\partial \mu}{\partial \rho} \right)_T \frac{H^2}{2} \right] = 0 \text{ as } \left(\frac{\partial \mu}{\partial \rho} \right)_T = 0 \tag{2.17}$$

Thus, substituting into (2.10)

$$f_m = -\nabla \mu \frac{H^2}{2} - \mu_0 M \nabla H + \mu_0 M \nabla H = -\nabla \mu \frac{H^2}{2} \tag{2.18}$$

The expressions for the magnetic force term is then ,

$$f_{m,x} = -\frac{\partial \mu}{\partial x} \frac{H^2}{2} ; \; f_{m,y} = -\frac{\partial \mu}{\partial y} \frac{H^2}{2} \tag{2.19}$$

It is seen that the magnetic body force for the case considered is attributable to the step change in μ at the interface.

2.1.3 Buoyancy term

To include the effect of gravity, the body force is given by:

$$f^g = -\rho g \, ,$$

where g is acting in the negative y direction. The Boussinesq approximation is applied, i.e. the density variation to temperature is neglected everywhere except where it appears as the buoyancy term. Thus:

$$\rho = \rho(1-\beta(T-T_0)), \text{ or}$$
$$f^{g} = -\rho(1-\beta(T-T_0))g \tag{2.24}$$

Substituting the body force terms, we obtain:

2.1.4 The Maxwell's equations

At this stage, for simplicity the study will cover non-conducting ferrofluids. For such fluids we have $\omega = 0$. The Maxwell's equations reduce to:

$$divB = 0$$
$$rotH = 0 \tag{2.25}$$

The magnetic induction B, the magnetic intensity H and the magnetization H are related by

$$B = \mu_0 (H + M) \tag{2.26}$$

Substituing (2.14) into (2.26)

$$B = \mu H \tag{2.27}$$

One can define a magnetic potential Φ which satisfies $H = \nabla\Phi$ (2.28)

Substituting (2.28), (2.27) into (2.25), the Maxwell's equation is obtained

$$\nabla \cdot \mu\nabla\Phi = 0 \tag{2.29}$$

The boundary conditions on the Maxwell's equation are:

$$(B_1 - B_2)\cdot n = 0$$
$$(H_1 - H_2)\times n = 0, \text{ where n is the normal at the interface}$$

Substituting the various terms into the original Governing equations of (2.1-2.8)

2.2 Two-layer fluid problem

The application considered mainly is the two immiscible fluid layers contained in a square box, subjected to a temperature gradient applied in the horizontal direction. The lower fluid is a ferrofluid (water based) while the upper fluid is a diamagnetic fluid, oil. The system is subjected to an external magnetic field gradient. The aspect ratio is kept constant, and the wall boundaries are solid. A schematic of the setup is shown in Fig. [2.1]

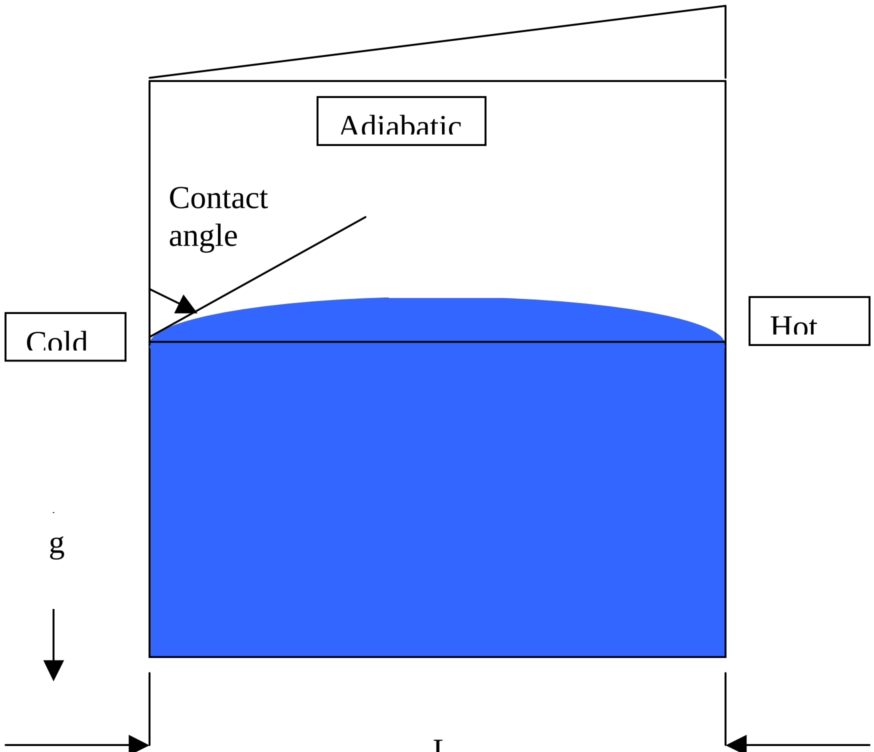

Fig. [1] A Schematic of the Two-layer problem

The non-dimensionalization is as follows

ρ	x	y	u	v	t	p	g	k	H	$T-T_0$	σ
ρ_{ref}	L	L	U	U	L/U	$\rho_{ref}U^2$	g_{ref}	$1/L$	H_0	∇T_{ref}	σ_{ref}

Table [1] non-dimensionalizing parameters

The final resulting equations (2.46-2.52) are then:

$$\frac{\partial \phi}{\partial t} + u\frac{\partial \phi}{\partial x} + v\frac{\partial \phi}{\partial y} = 0$$

$$\frac{\partial u}{\partial x} + \frac{\partial v}{\partial y} = 0$$

$$\frac{\partial u}{\partial t} + u\frac{\partial u}{\partial x} + v\frac{\partial u}{\partial y} = -\frac{1}{\rho(\phi)}\frac{\partial p}{\partial x} + \frac{1}{\boldsymbol{Re}}\frac{1}{\rho(\phi)}\frac{\partial}{\partial x}\left(\eta(\phi)\frac{\partial u}{\partial x}\right) + \frac{1}{\boldsymbol{Re}}\frac{1}{\rho(\phi)}\frac{\partial}{\partial y}\left(\eta(\phi)\frac{\partial u}{\partial y}\right)$$
$$-\frac{\boldsymbol{Bom}}{\boldsymbol{We}}\frac{1}{\rho(\phi)}\left(\frac{\mu_2}{\mu_0} - \frac{\mu_1}{\mu_0}\right)\delta(\phi)\frac{d\phi}{dx}H^2 - \frac{1}{\boldsymbol{We}}\frac{1}{\rho(\phi)}\left(\nabla\cdot\frac{\nabla\phi}{|\nabla\phi|}\bigg|_{\phi=0}\right)\frac{\partial \phi}{\partial x}\delta(\phi)$$
$$+\frac{\boldsymbol{Ma}}{\boldsymbol{Pr}\ \boldsymbol{Re}^2}\frac{T}{\rho(\phi)}\left(\nabla\cdot\frac{\nabla\phi}{|\nabla\phi|}\bigg|_{\phi=0}\right)\frac{\partial \phi}{\partial x}\delta(\phi)$$

$$\frac{\partial v}{\partial t} + u\frac{\partial v}{\partial x} + v\frac{\partial v}{\partial y} = -\frac{1}{\rho(\phi)}\frac{\partial p}{\partial y} + \frac{1}{\boldsymbol{Re}}\frac{1}{\rho(\phi)}\frac{\partial}{\partial x}\left(\eta(\phi)\frac{\partial v}{\partial x}\right) + \frac{1}{\boldsymbol{Re}}\frac{1}{\rho(\phi)}\frac{\partial}{\partial y}\left(\eta(\phi)\frac{\partial v}{\partial y}\right)$$
$$-\frac{\boldsymbol{Bom}}{\boldsymbol{We}}\frac{1}{\rho(\phi)}\left(\frac{\mu_2}{\mu_0} - \frac{\mu_1}{\mu_0}\right)\delta(\phi)\frac{d\phi}{dy}H^2 - \frac{1}{\boldsymbol{We}}\frac{1}{\rho(\phi)}\left(\nabla\cdot\frac{\nabla\phi}{|\nabla\phi|}\bigg|_{\phi=0}\right)\frac{\partial \phi}{\partial y}\delta(\phi)$$
$$+\frac{\boldsymbol{Ma}}{\boldsymbol{Pr}\ \boldsymbol{Re}^2}\frac{T}{\rho(\phi)}\left(\nabla\cdot\frac{\nabla\phi}{|\nabla\phi|}\bigg|_{\phi=0}\right)\frac{\partial \phi}{\partial y}\delta(\phi) - \frac{1}{\boldsymbol{Fr}} + \frac{\boldsymbol{Gr}}{\boldsymbol{Re}^2}\beta(\phi)T$$

$$\frac{\partial q}{\partial t} + u\frac{\partial q}{\partial x} + v\frac{\partial q}{\partial y} = \frac{1}{\boldsymbol{Pe}}\left[\frac{\partial}{\partial x}\left(\kappa\frac{\partial T}{\partial x}\right) + \frac{\partial}{\partial y}\left(\kappa\frac{\partial T}{\partial y}\right)\right]$$

$$\frac{\partial}{\partial x}\left(\mu\frac{\partial \Phi}{\partial x}\right) + \frac{\partial}{\partial y}\left(\mu\frac{\partial \Phi}{\partial y}\right) = 0$$
$$H = \frac{\partial \Phi}{\partial x}i + \frac{\partial \Phi}{\partial y}j$$

where,

$$\boldsymbol{Re} = \frac{\rho_{ref}UL}{\eta_{ref}};\boldsymbol{We} = \frac{\rho_{ref}U^2L}{\sigma_{ref}};\boldsymbol{Gr} = \frac{\rho_{ref}{}^2 g_{ref}\beta\Delta TL^3}{\eta_{ref}{}^2};\boldsymbol{Bo_m} = \frac{\mu_0 H_0{}^2 L}{2\sigma_{ref}};$$

$$\boldsymbol{Pr} = \frac{\eta_{ref}C_p}{\kappa};\boldsymbol{Fr} = \frac{U^2}{g_{ref}L};\boldsymbol{Ma} = \frac{\rho_{ref}C_p\gamma\Delta TL}{\eta_{ref}\kappa},$$ and

$$\rho(\varphi) = 1 + (1 - \frac{\rho_2}{\rho_1})He(\phi);$$

$$\mu(\phi) = \frac{\mu_1}{\mu_0} + (\frac{\mu_1}{\mu_0} - \frac{\mu_2}{\mu_0})He(\phi); \quad \beta(\phi) = 1 + (1 - \frac{\beta_2}{\beta_1})He(\phi)$$

Typical Material properties

	1-Ferrofluid (water based)	2- Shell Oil
ρ	*1380 kg/m³*	*800 kg/m³*
κ	*2.7 W/m K*	*0.122 W/m K*
C_p	*3000 J/kg K*	*2038 J/kg K*
η	*0.00664 kg/ms*	*0.00381 kg/ms*
σ	*0.00307 kg/s²*	*0.00307 kg/s²*
β	*0.000260 (1/K)*	*0.000717 (1/K)*
μ / μ_0	*3.2*	*1.0*

Table [2] Typical material properties of Ferrofluid and diamagnetic fluid

The velocity scale is chosen to be $U = \frac{\gamma \Delta T}{\eta_{ref}}$;

$L = .005m; \quad g_{ref} = 9.81 m/s^2; \quad H_0 = 2400 Amp/m; \quad \Delta T = 100^\circ K$

Taking the material properties of the ferrofluid as the reference, the non-dimensional parameters are obtained follows for the typical base solution:

	Re	***We***	***Gr***	***Bo$_m$***	***Pr***	***Fr***	***Ma***
Two-layer	135.542	33.3979	1805.22	5.89415	7.3778	0.2646	1000.0

Table [3] Typical values of Non-dimensional parameters

The boundary conditions:
Isothermal boundary conditions on the left and right walls
(T=0 & T=1 respectively)
and adiabatic upper and lower walls ($T_n=0$).
The boundary conditions on Φ derived from (2.25) are:

$$\frac{\partial \Phi}{\partial x} = 0; \quad \frac{\partial \Phi}{\partial y} = \frac{\mu_0}{\mu_1} H_0; \quad \text{Upper wall}$$

$$\frac{\partial \Phi}{\partial x} = 0; \quad \frac{\partial \Phi}{\partial y} = H_0; \quad \text{Left \& Right wall}$$

$$\frac{\partial \Phi}{\partial x} = 0; \quad \frac{\partial \Phi}{\partial y} = \frac{\mu_0}{\mu_2} H_0; \quad \text{Lower wall}$$

Finally, a contact angle is specified at the intersection of the interface and the sidewalls, to complete the boundary conditions for the problem.

3 Results

The results from the two-fluid layer described in Section 2, is now presented. The first effect studied is that of, the magnetic field on the thermo-capillary flow. Thus, the Magnetic field is increased over different Marangoni numbers, and the behavior of the two-fluid system is studied, in particular we track:

- -The maximum velocity in the system
- -The maximum local velocity near the interface.
- -The heat diffusion across the interface per unit volume.

The gravity is completely eliminated as the thermo-capillary effects are particularly sought out. Thus Fr= infinity and Gr=0. The other non-dimensional parameters are:

Ar=1, Pr=7.37, Re=200, We=33, Contact angle=67.5

The Marangoni number is varied from 10,100,1000. Bo_m is varied from 0 to 0.5.

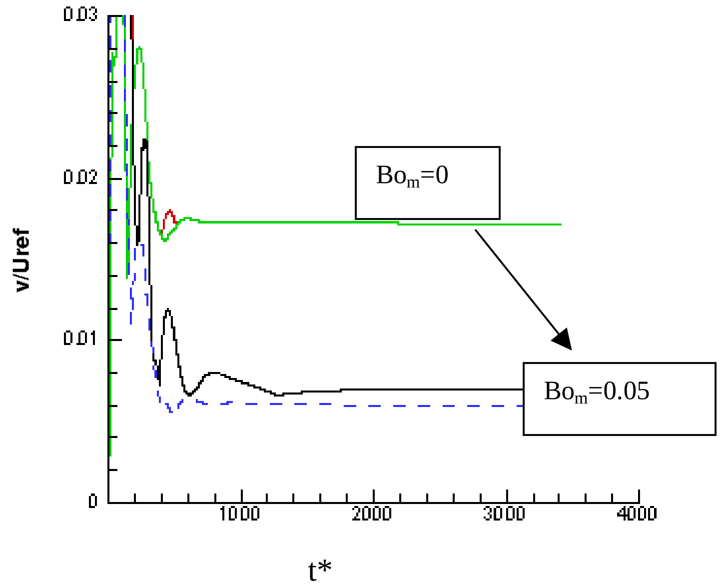

Fig. 2 The maximum velocities globally and locally vs. t* for (a) Bo_m=0 and (b) Bo_m=0.05 for Ma=100

The benefit of the magnetic field is seen instantly from Fig.2. On the application of a Bo_m=0.05, both the global and local and velocities fall by almost 50%. This indicates immense potential for the use of magnetic fields in curbing the convective velocities due to thermo-capillary effects. The applicability range is now studied.

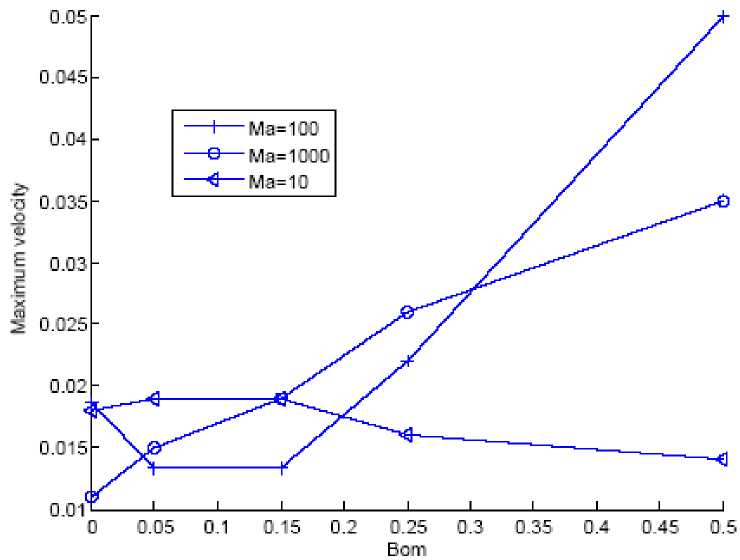

Fig. 3 The maximum velocities globally vs. Bo_m for Ma=10,100,1000

From the parameter space chosen, a number of effects can be seen from Fig. 3. Firstly, for the lowest Marangoni number, the maximum velocity actually increases and then decreases with increasing Bo_m, indicating that it takes more magnetic field strength for the stabilizing effect of the magnetic field to register. However, for a higher Marangoni number of 100, the velocity immediately decreases and reaches an optimum at Bo_m=0.15, after which the magnetic field stabilizing effect begins to wane. For higher Marangoni numbers (1000 or more) the maximum velocity almost monotonically increases with the magnetic field, having no stabilizing effect whatsoever. It would appear that applying an external magnetic field would have no role to play in stabilizing thermocapillary flows of Ma>1000, However more interesting patterns are seen from the local velocity variation in Fig.4.

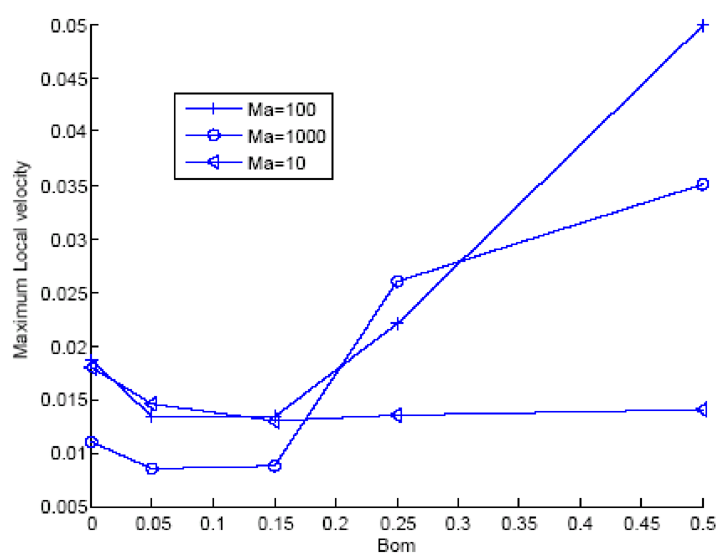

Fig. 4: The maximum velocities locally vs. Bo_m for Ma=10,100,1000

The effect seen is that for almost all the Ma, the local velocity decreases with increasing Bo_m. This suggests that velocities away from the local area of interest play a major role in increasing the convective velocities. However in cases where the velocities away from the area of interest are not significant, the application of the magnetic field could render beneficial results.
From Fig.5, there are even more beneficial results seen from the application of the magnetic field. For all the Ma chosen, the heat flux across the interface dramatically decreases. In crystal growth applications, this is a highly desirable feature.

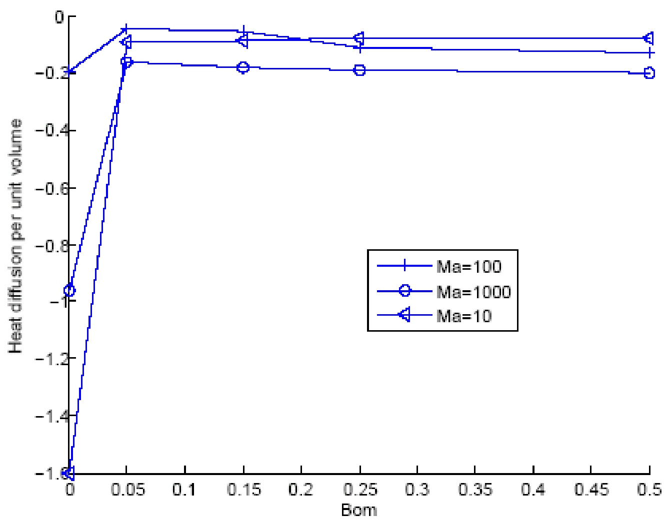

Fig. 5: The maximum velocities locally vs. Bo_m for Ma=10, 100, 1000

In summary, the magnetic field coupled with the ferrofluid has a very significant effect in reducing the convective velocities of the system, and there is indeed immense potential of using such a technique, based on the simulations conducted in this study.

To gain further insight into the mechanism of the convective velocities, the velocity contours are studied next.

Figure 6a-c shows u-velocity contours for Ma=10 at 3 different Bo_m's. The temperature contours are neglected as it is almost identical to the conduction solution for all these cases. For Bo_m=0, if the interface, as indicated in Fig. 6-a is noticed, there are some roll structures seen in the upper diamagnetic fluid phase, while in the lower ferrofluid there are well defined cellular structures.

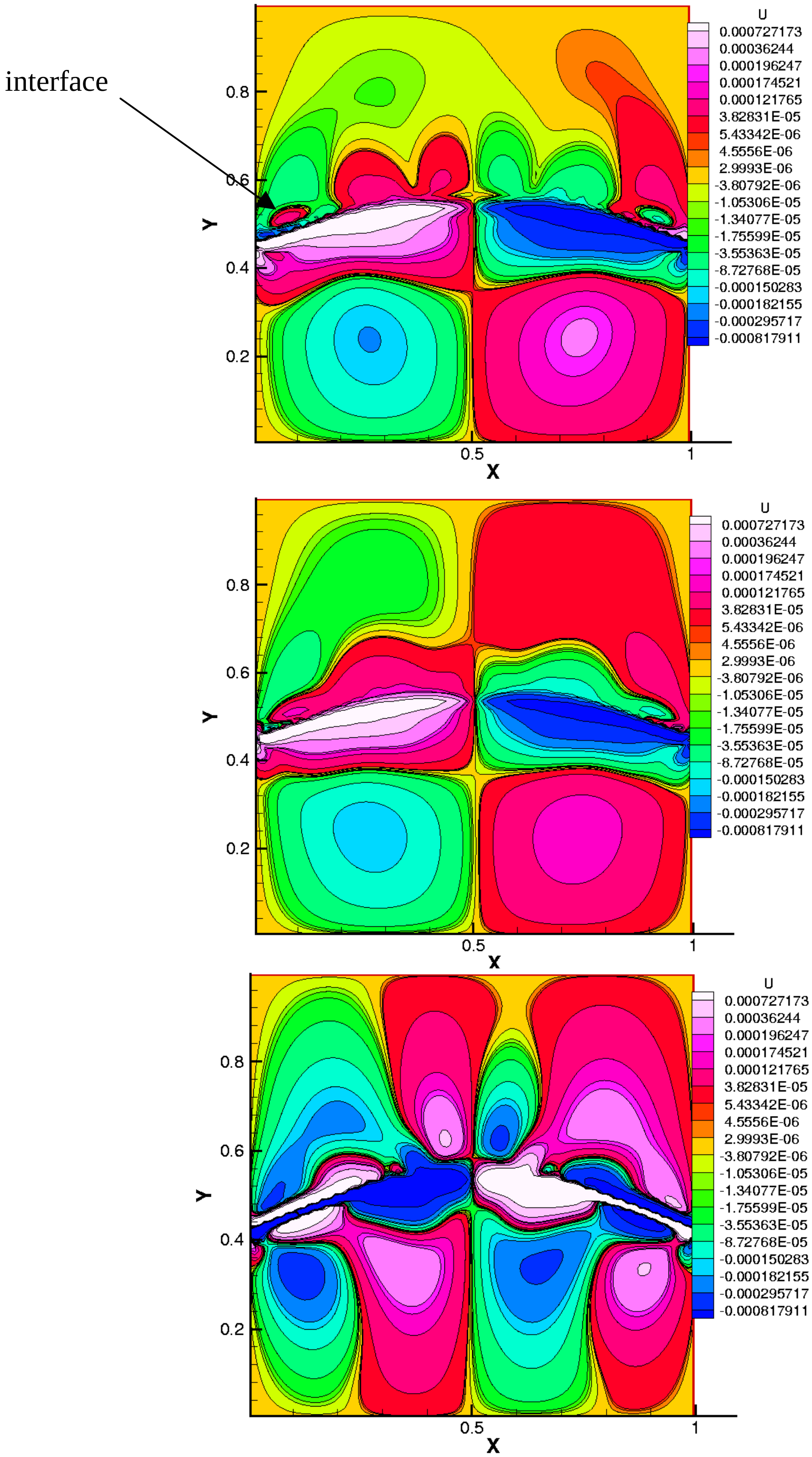

Fig.6a-c: Streamwise velocity contours for Ma=10, (a) Bo_m = 0, (b) Bo_m =0.05, (c) Bo_m=0.5

The interface consists of fluids having different properties with a constant shear force acting on it, which is why the irregular patterns are seen. However, with the addition of the magnetic field, we see the disappearance of these irregularities in Fig. 6-b and see well defined cellular structures even in the diamagnetic fluid.
Recalling Equation (2.37-38) the force due to the magnetic field is a surface force due to the step change in the magnetic permeability. It is proposed here that it is this surface density force which is primarily responsible for suppressing the instabilities, for the given configuration.
On further increasing Bo_m, we see in Fig. 6-c the flow went through an instability to bifurcate into multi-cellular structures. This is accompanied by an increased curvature of the interface. A similar behavior is witness for the Ma=100 case in Fig. 7a-c

For Ma=1000, the existence temperature gradients at the interface are seen for the first time. For the Bo_m =0 case, the gradients are sufficiently discernable. On increasing the magnetic field, we see the temperature contours “straightening out”. This helps understanding how the heat flux gets so dramatically reduced with increased magnetic field. It is also noticed that at Bo_m =0.5 the cell has not bifurcated into cellular structures. Thus the Marangoni number has an important role to play in this phenomenon.

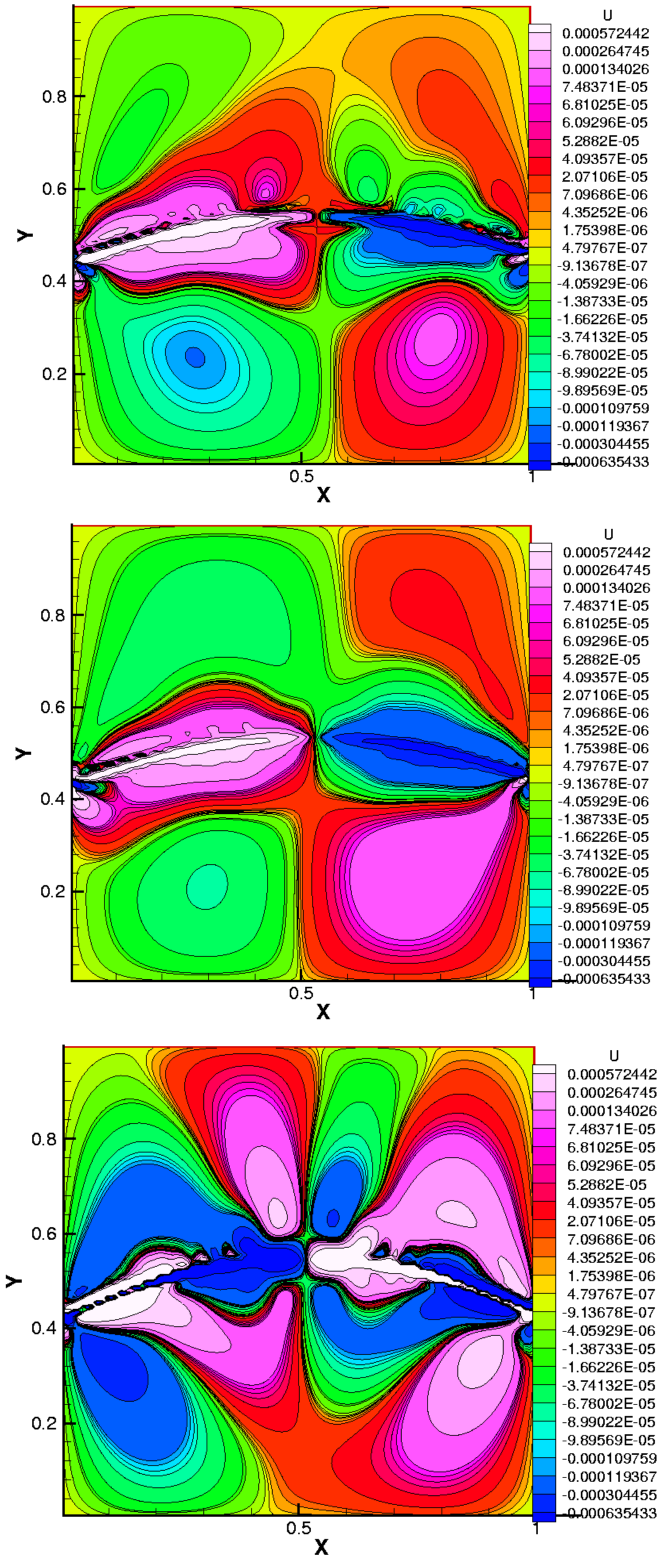

Fig.7-a-c: Streamwise velocity contours for Ma=100, (a) Bo_m = 0, (b) Bo_m =0.05, (c) Bo_m=0.5

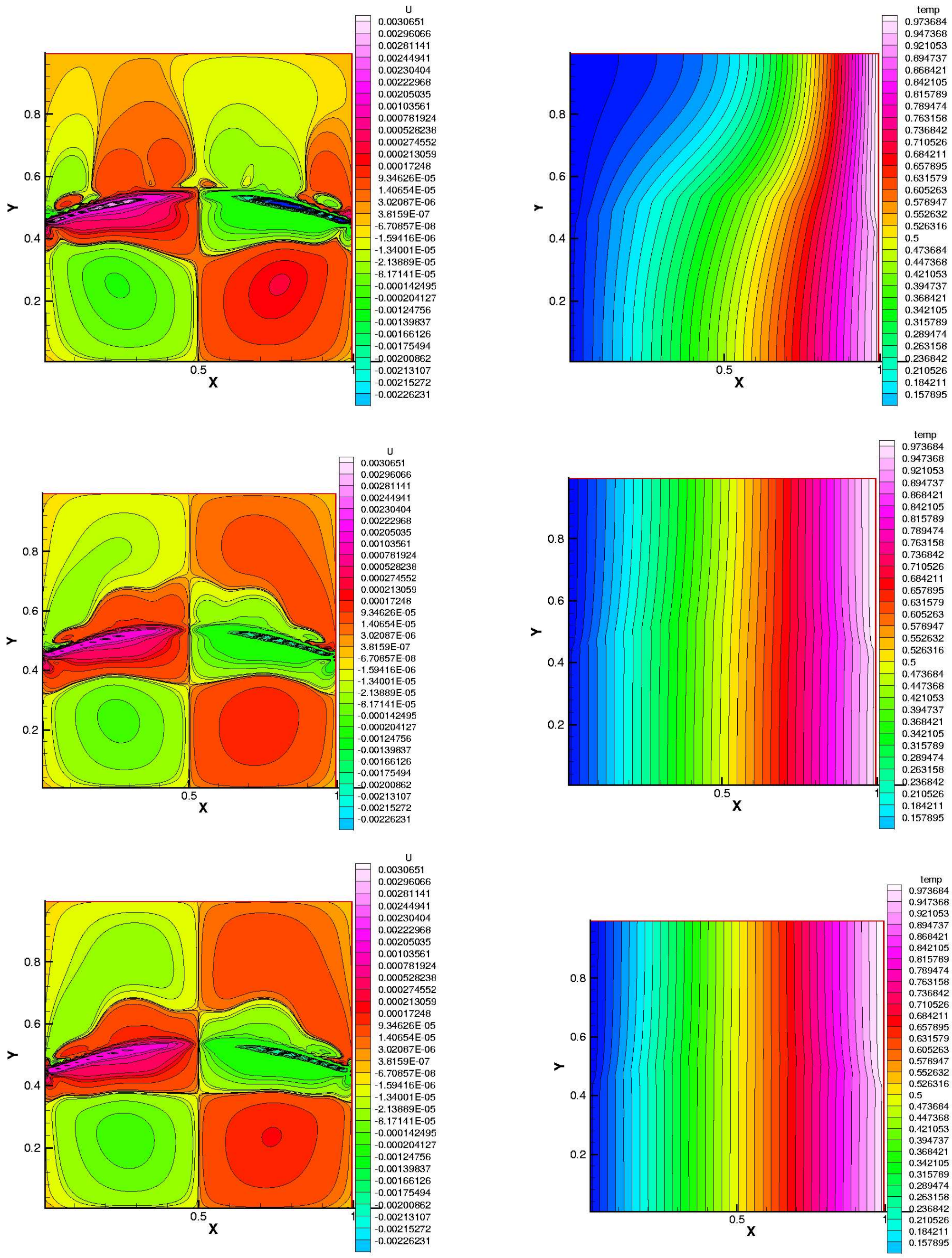

Fig. 8a-c: Streamwise velocity contours for Ma=1000, (a) $Bo_m = 0$, (b) $Bo_m = 0.05$, (c) $Bo_m = 0.5$

3.2 Two fluid-layer, Mixed Thermo-capillary Buoyancy effects

In the next set of simulations, the effect of gravity of 3 levels are investigated and it is to be seen whether the magnetic field has any effect on the velocities in such cases. This is in addition to the thermo-capillary effect.

The parameters chosen are:

Aspect ratio=1, Gr=1805, Pr=7.37, Re=135, We=33, Ma=1000, alpha=67.5 (Fr = 100000, 1000, l0)

Bo_m=0 - 0.5

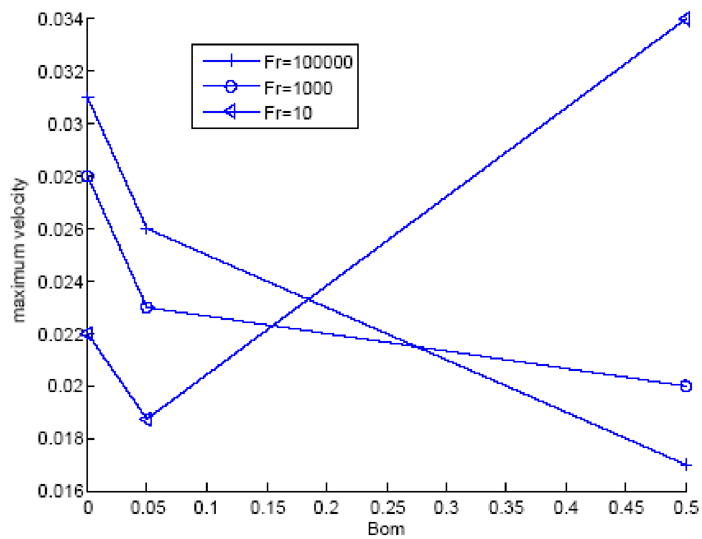

Fig. 9 Maximum global velocity vs. Bo_m, Fr = 100000, 1000, l0

From Fig. 9, 10, once again the maximum velocity is found to decrease with increasing $Bo_{m.}$. However the mechanism which causes this is different from that in the thermo-capillary case.

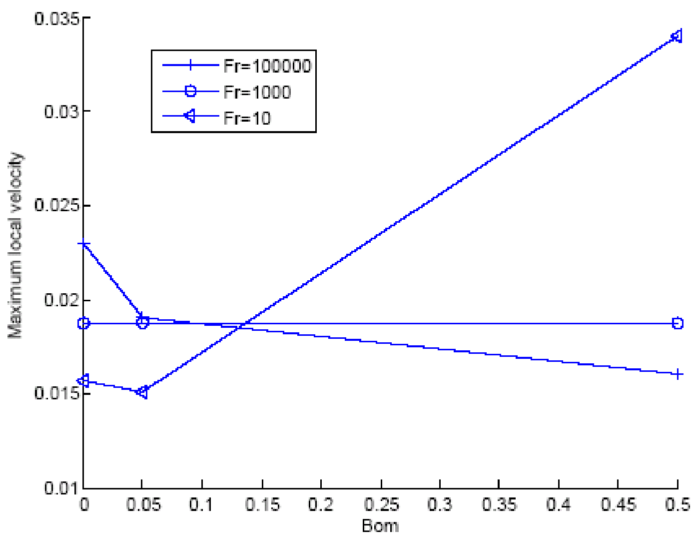

Fig. 10: Maximum local velocity vs. Bo_m, Fr = 100000, 1000, l0

Unlike in the thermo-capillary case, the velocity contours show a smooth pattern in the upper and lower phases. Figure 11 shows the u-velocity contours for Fr=1000,

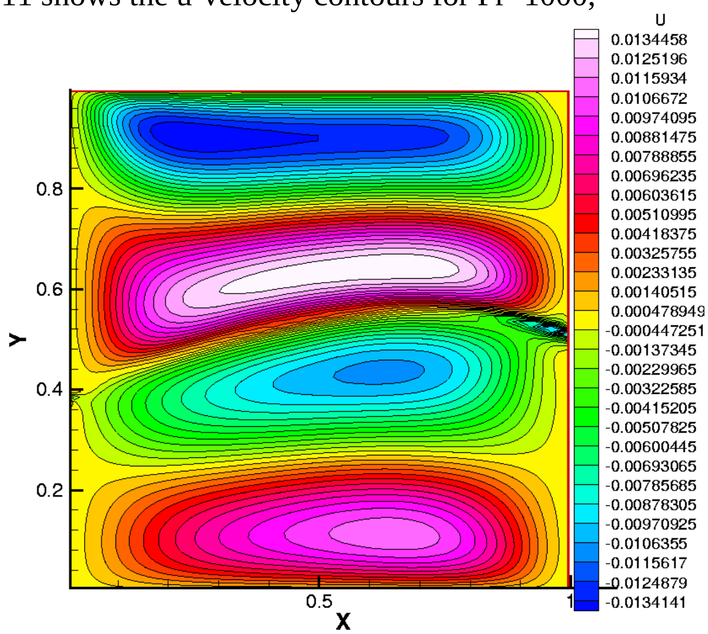

Fig. 11: U velocity contours, Fr=1000

The effect of the magnetic field can be best understood by seeing it's effect on the interface shape. Fig 12a-c show the interfaces and it's adjoining temperature contours.

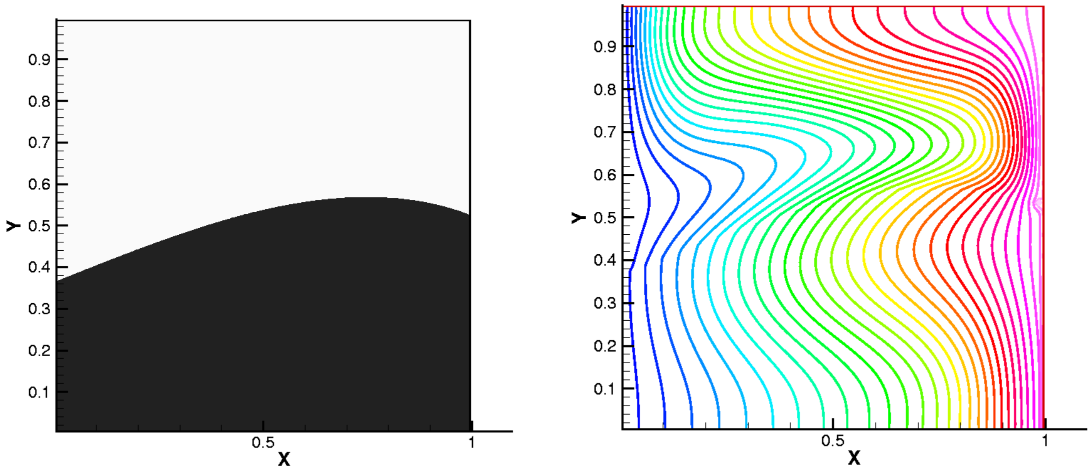

Fig. 12-a Interface and temperature contours, Bo_m=0, Fr=1000

In Fig 12-a above, Bo_m =0. This is the base state solution. Due to the effect of the gravity and Grashof number, the interface is no longer symmetrical as there is buoyancy driven convection going on the cell.

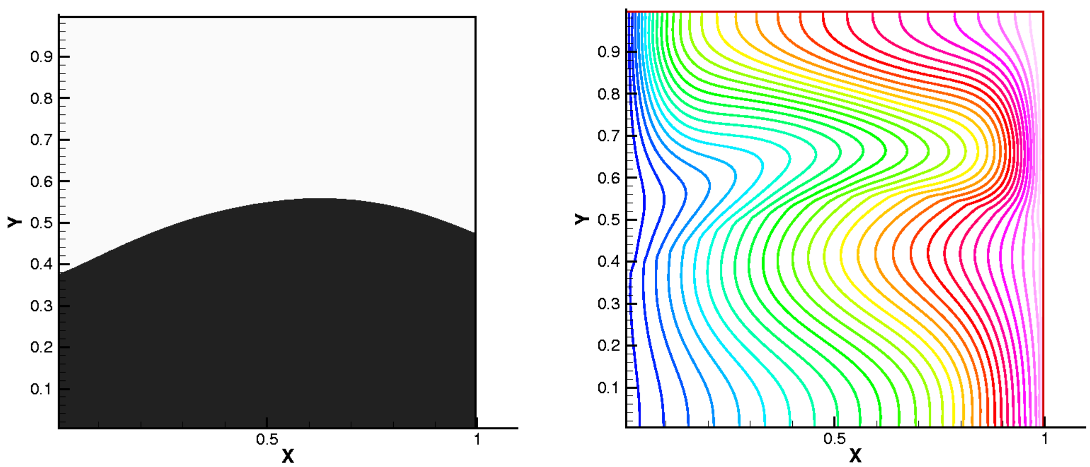

Fig. [5.21b] Interface and temperature contours, Bo_m=0.05, Fr=1000

In Fig. 12-b above, Bo_m =0.05 The effect of the magnetic field is to shift the maxima of the interface towards the center. This affects the curvature of the interface which consequently changes the interface region velocities. This is the stabilizing effect of the magnetic field in this case.

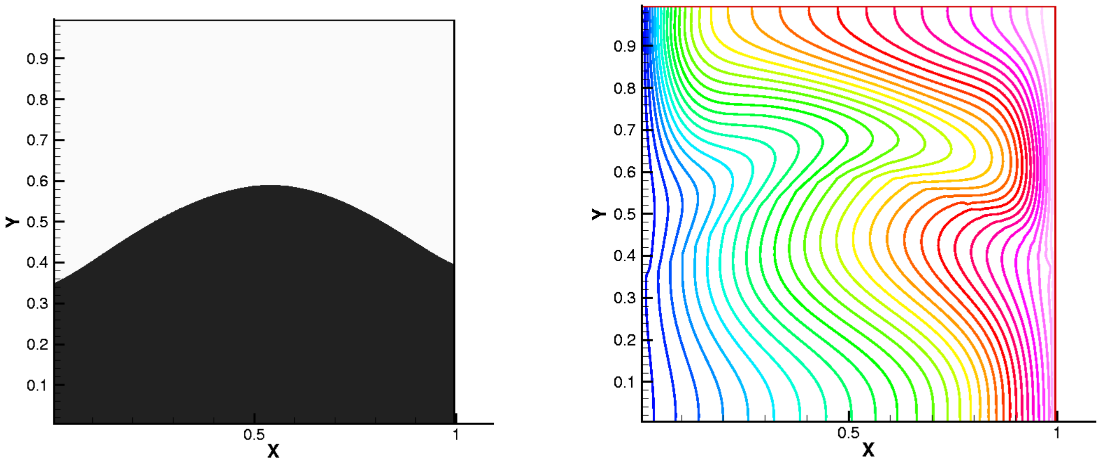

Fig. 12-c: Interface and temperature contours, Bo_m=0.5, Fr=1000

However this may not always hold true. In the Fig. 12-c above, the curvature has significantly changed to increase the convective velocities. This could be the effect of the significant temperature gradients which were virtually absent in the thermo-capillary case. It is also to be seen that due to these significant temperature gradients, the diffusive fluxes are not much affected by the magnetic field as seen in Fig. 13.

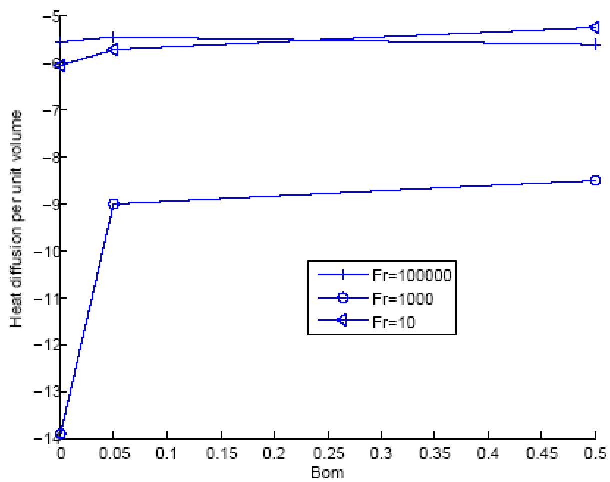

Fig. 13: Heat diffusion vs. Bo_m, Fr = 100000, 1000, l0

3.3 Two-fluid layer Instability

Noticing in Fig. 12-a the significant angle that the steady state interface makes with the horizontal, it was found that on increasing the Grashof number, the angle the interface makes with the horizontal keeps increasing. Fig. 14-a shows the steady state interface at for Fr=1000 at

Gr=6305. This was found to be the critical Grashof number at this Fr. On increasing Gr, the flow was found to undertake revolutions and thus become unstable, as in Fig. 14-b. A Stability curves is thus constructed in the Gr vs. Fr space and shown in Fig. 15. The critical Gr number falls rapidly with the increasing Fr number upto 100, after which there is less effect of Fr.

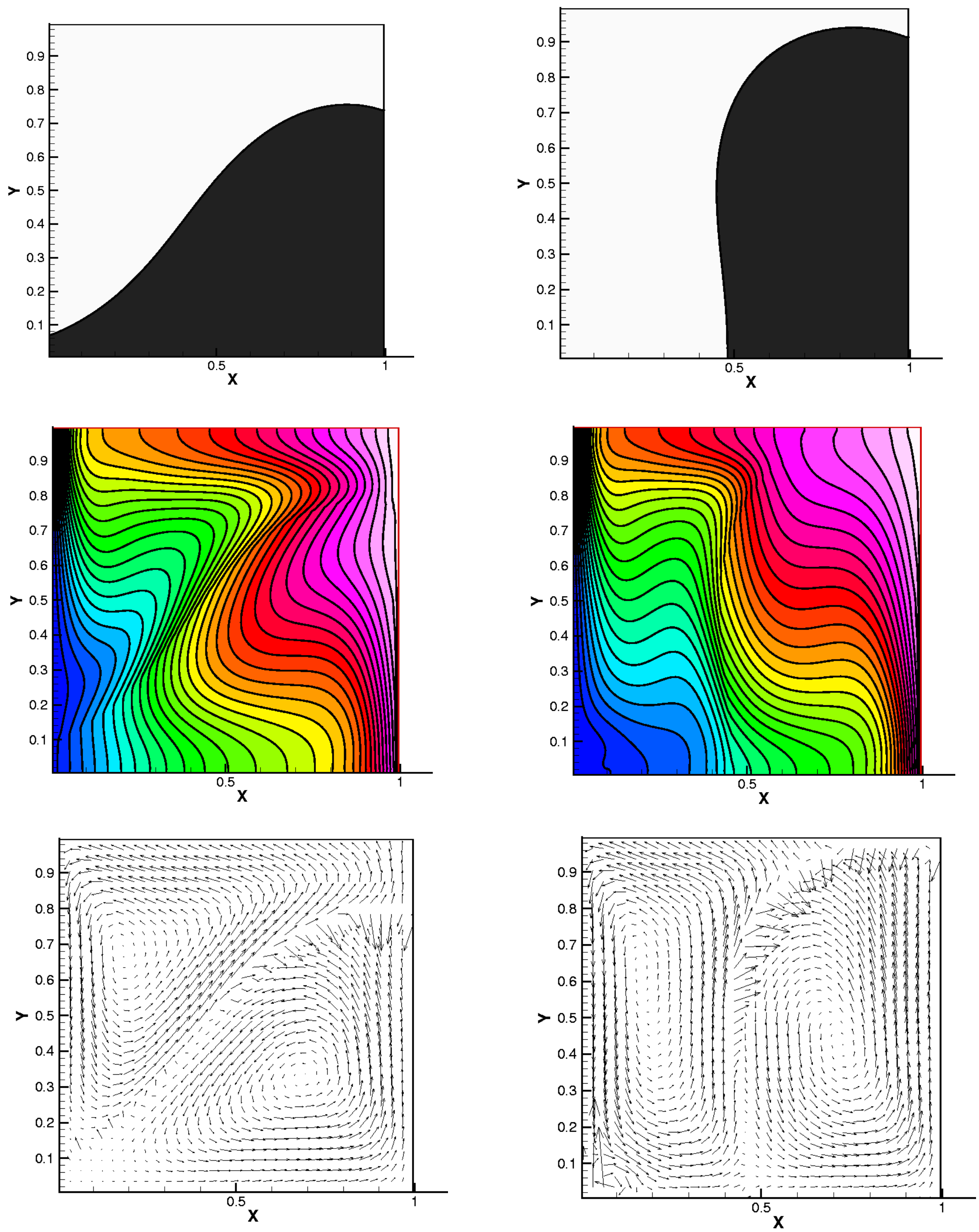

(a) (b)

Fig. 14: Oscillating Two-layer flow: Temperature and velocity vectors at (a) Fr=1000, Gr=6305; (b) Gr>6305

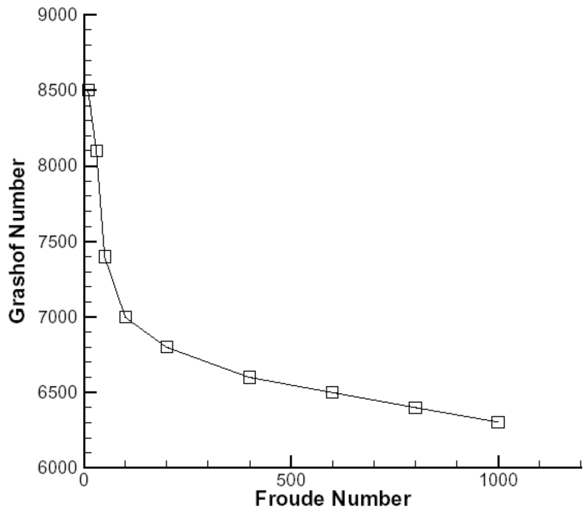

Fig. 15: Neutral stability curve in the Gr vs. Fr number space.

3.4 Weber Number Effect

Figure 16 shows the effect of increasing the magnetic field on the local velocity, for different Weber numbers, indicative of varying magnitudes of the surface tension between the participating fluids. It is uniformly seen that the magnetic field decreases the convective velocities. However, from the Fig. 16 it is noticed that there is more significant drop in the velocities at lower We (higher surface tension) that at higher We. Thus the effect of the magnetic field is best seen at lower We (0~40).

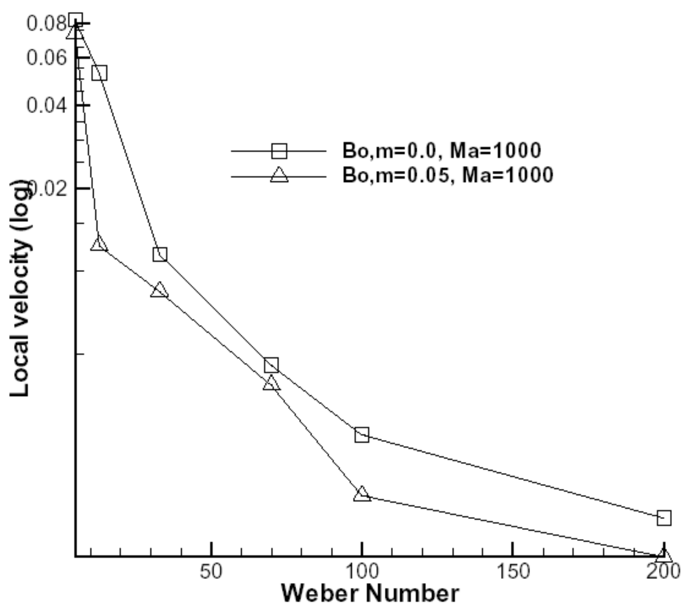

Fig. 16: Weber number effect

3.5 Convective Heat Transfer

Figures 17-20 show the change of the Convective Heat transfer over a parameter space of the Marangoni, Froude and Grashof Numbers. Since CHT is a vector, the values in the x- direction and y-direction are separately shown. The variation of CHT is found to be non-trivial, for example in Fig. 17, while for 0 Grashof number, over a range of Ma the CHT in the x-direction is uniformly and monotonically increasing, it is seen that for non-zero Gr, there is a slight dip in the CHT and then it increases with magnetic field. The same effect is noticed for the CHT in the y-direction (Fig. 18). The Froude number effect Figs. 19-20 is found to dampen the effect of the magnetic field. Thus it is seen that for very high Fr, the magnetic field has less of an effect on curbing/enhancing the Convective Heat Transfer.

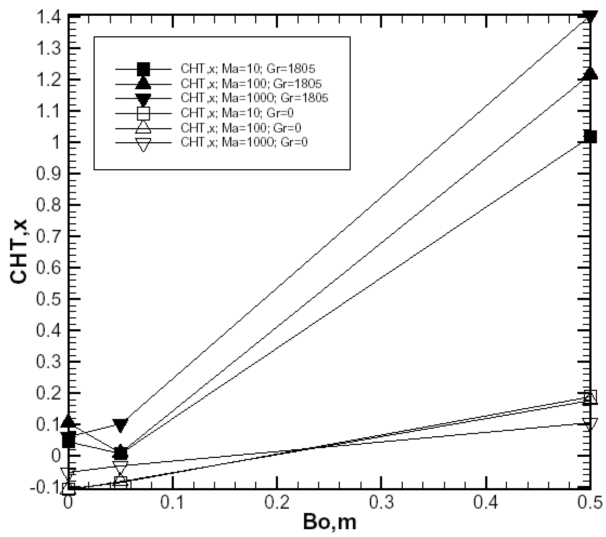

Fig. 17: Convective Heat transfer in the x- direction as a function of Magnetic Bond number for Gr=0; Gr=1805 over a range of Marangoni numbers.

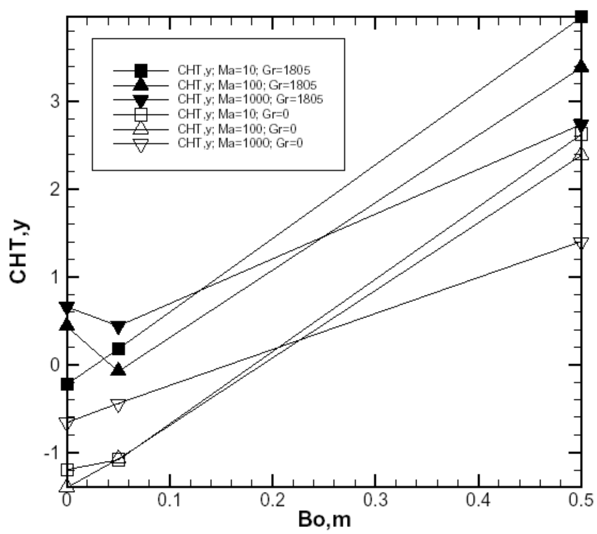

Fig. 18: Convective Heat transfer in the y- direction as a function of Magnetic Bond number for Gr=0; Gr=1805 over a range of Marangoni numbers.

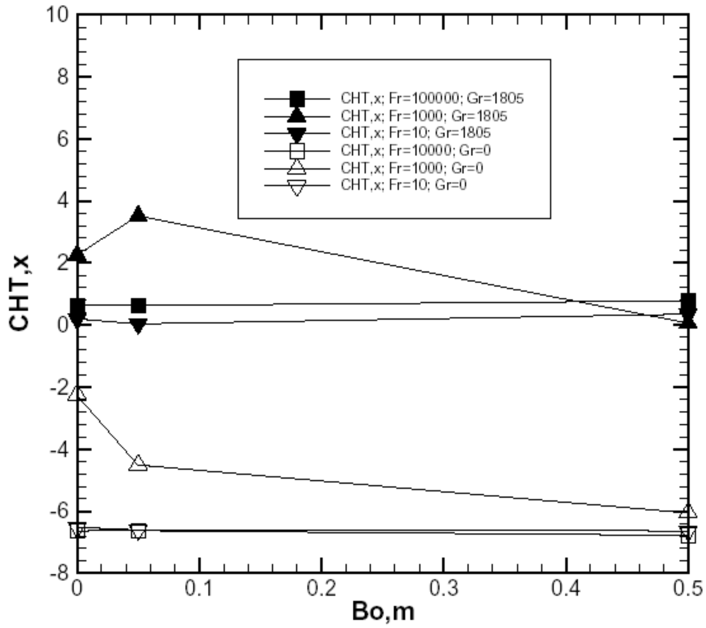

Fig. 19: Convective Heat transfer in the x- direction as a function of Magnetic Bond number for Gr=0; Gr=1805 over a range of Froude numbers.

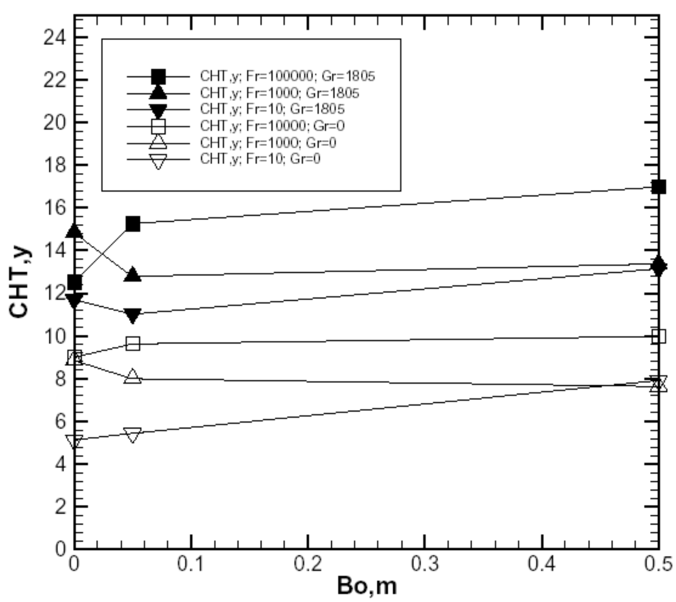

Fig. 20: Convective Heat transfer in the y- direction as a function of Magnetic Bond number for Gr=0; Gr=1805 over a range of Froude numbers.

3.6 Contact Angle Effect

The simulations presented so far have been done assuming a constant contact angle at the wall to be 67.5. It is to be seen whether for different contact angles there is a change in the beneficial effects of magnetic field. Interesting phenomenon are noticed in Fig. 21. where the global velocity is varied for different contact angles and different Bo,m. It is seen that at higher Gr, the magnetic field still has a beneficial effect, but this is valid only for a concave interface (i.e contact angle > 90). For a convex interface, increasing the magnetic field increases the velocity. This trend is noticed even at non-zero Gr. In Fig 22, higher Ma tend to give a lower velocity for certain magnetic fields. This trend was seen initially in Fig 2. The reduced effect of magnetic field for convex interfaces is once again seen from Fig. 22. Thus there is strong dependence on the contact angle. Figure 23 shows that with increasing Gr, at a constant magnetic field, the convective velocities increase significantly. However it is interesting to see that these velocities reduce with increasing Marangoni number when the interface is concave (and vice versa when convex). The velocities are further reduced as the contact angle tends to 90, and the effect of the Marangoni number seems to be more pronounced at such contact angles. Figure 24 shows that uniformly the velocities decrease with increasing Froude number, whether a concave or a convex interface. The effect of the contact angle on the convective heat transfer is next seen. In Figure 25, it seen that the CHT is reduced only slightly with increasing magnetic field for the Gr=0 and concave interface. For all other cases the CHT was seen to increase.

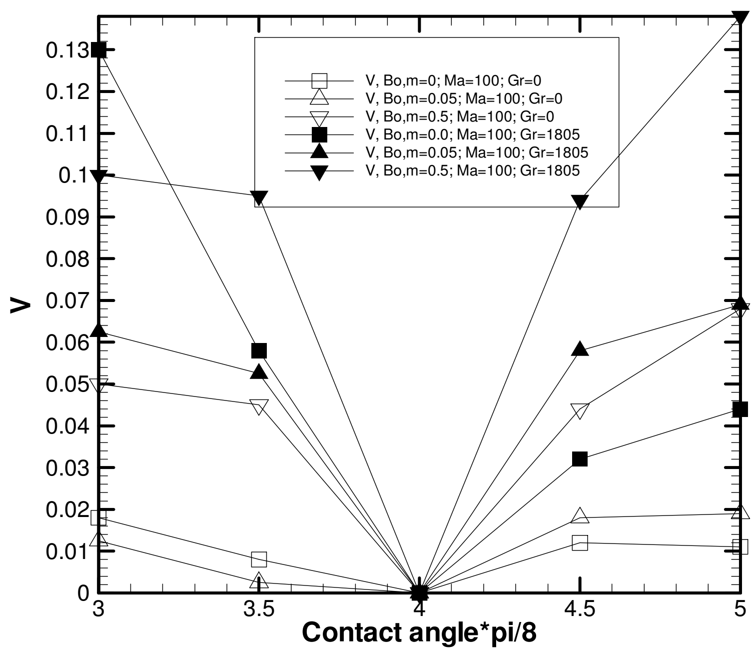

Fig. 21: Global velocity vs. Contact angle at constant Ma, and 2 different Gr.

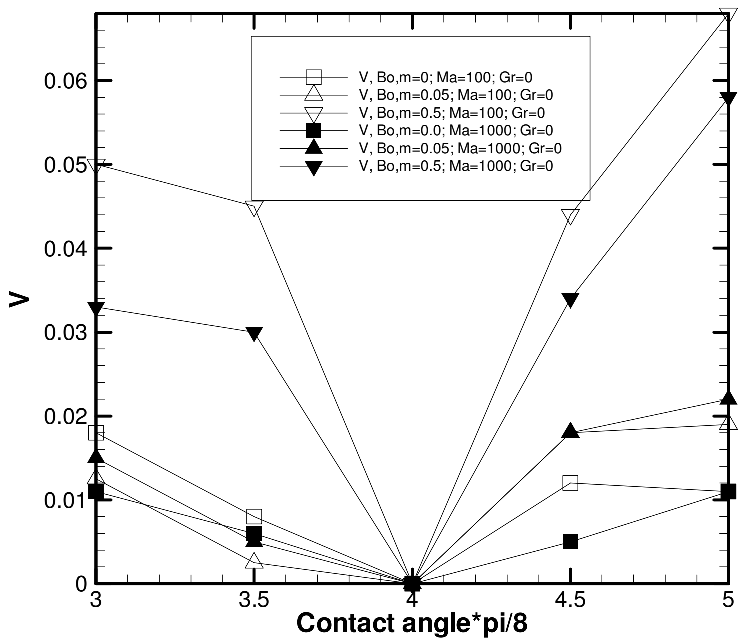

Fig. 22: Global velocity vs. Contact angle at constant Gr=0, and 2 different Ma.

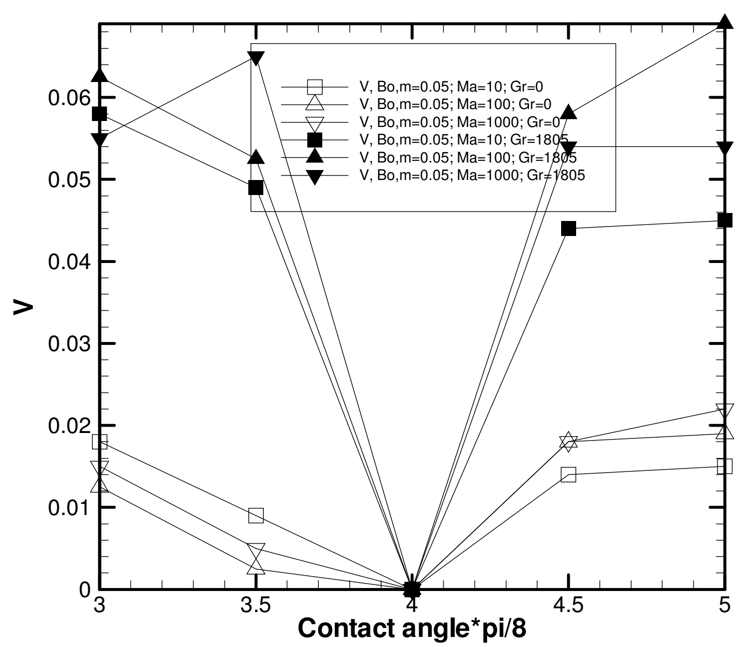

Fig. 23: Global velocity vs. Contact angle over a range of Marangoni numbers and at constant External Magnetic Field, and 2 different Gr.

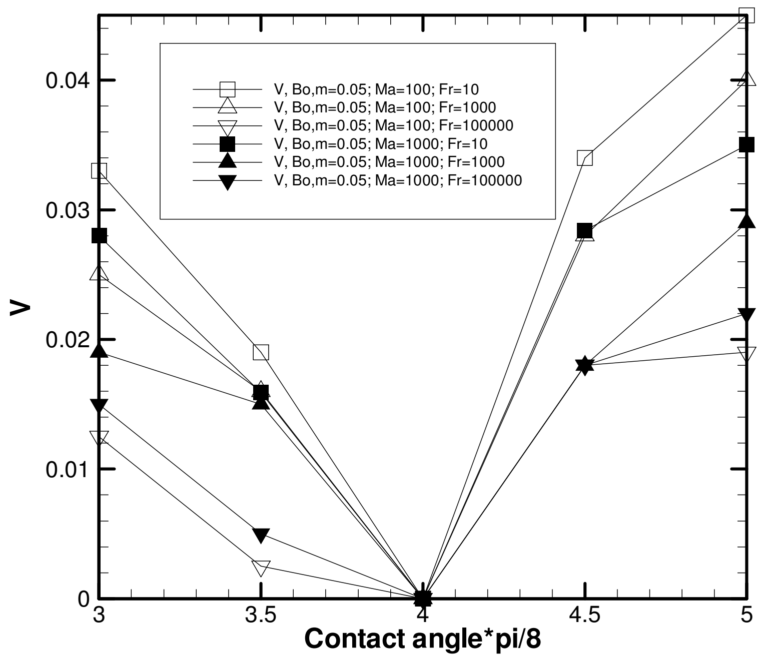

Fig 24: Global velocity vs. Contact angle over a range of Froude numbers and at constant External Magnetic Field, and 2 different Ma.

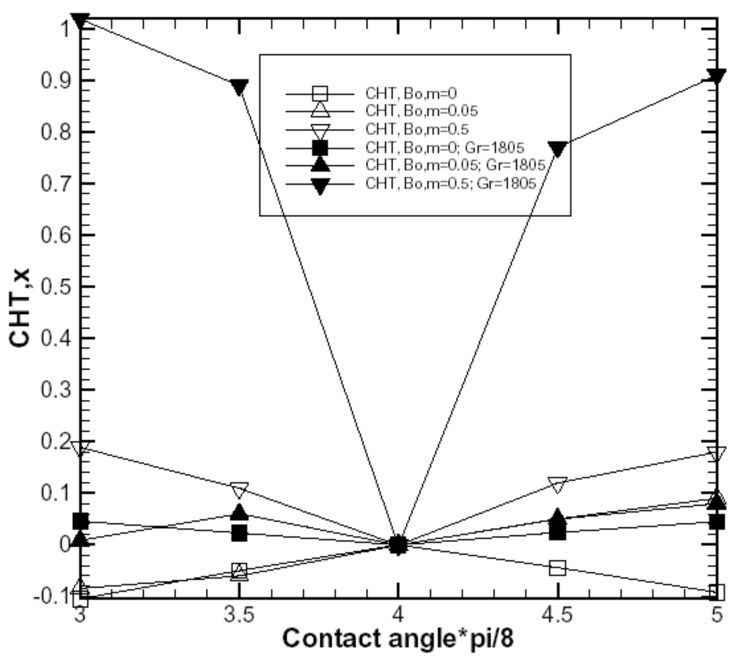

Fig. 25: Convective velocity vs. Contact angle over a range of magnetic field and at constant Ma=10, and 2 different Gr.

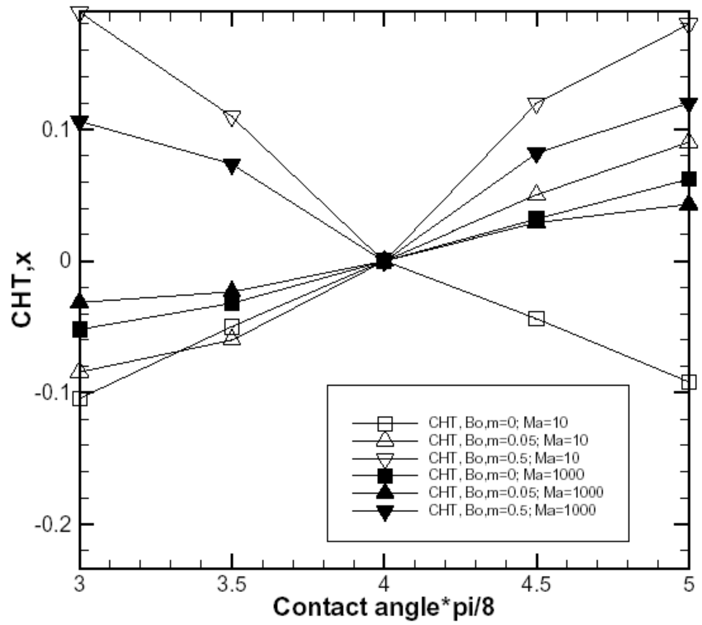

Fig. 26: Convective velocity vs. Contact angle over a range of magnetic field and at constant Gr=0, and 2 different Ma.

4. Concluding remarks

In this study, a novel numerical framework using state-of –the-art interface capturing numerical techniques, has been used to simulate a two-layer fluid problem and very interesting physical properties were demonstrated pertinent to the application of interest. It was found that the interface properties of a magnetic fluid can be used to reduce and control the convection in a fluid system under the influence of a magnetic field inside certain regimes of the Magnetic Bond number and the Marangoni number.

The results of the present investigation on reduction or otherwise of the convective flow velocity and heat transfer under certain conditions and certain values of the parameters indicates that the present method of approach and the associated modeling and numerical calculation can be useful to be employed or extended in the problems in crystal growth applications for control of convective flows, in particular, where convection can cause undesirable motions in the melt resulting in higher defect densities, improper mixing and non-uniform properties of the produced crystals.

A reader may get an impression that the results presented in the present paper are strictly applicable to situations where the fluid flows lack three dimensionality, as in the case of flow in a Hele-Shaw cell, for example. Although this can be true, it should be noted that the present model can also model many quasi-three dimensional flow cases where the flow depends weakly in a third dimension z and flow velocity is quite small in the z-direction. In addition, it should be noted that the present investigation of such two-dimensional model was needed as a first step in understanding the roles plays by the magnetic fluids and fields in flow controls aspects, which may be needed in the pratical and technological applications. The presents two-dimensional results can also stimulate future three-dimensional development of similar numerical techniques and subsequent three-dimensional studies in problems in various applications.

Other possible extensions of the present problem, which can be left to future work, include flow optimum control studies using a combination of vertical and transverse magnetic fields in static and dynamic states acting on multi-layer systems composed of ferrofluid and working fluid layers. It would be of interest to search for the most effective possible ways in three-dimensional systems where convective flow could be controlled especially in a microgravity environment, which could help to produce high quality materials, for example.

References

AULISA E, MANSERVISI S, SCARDOVELLI R, *et al.* 2003 A geometrical area-preserving Volume-of-Fluid advection method. Journal of Computational Physics 192 (1), 355-364.

BHATTACHARJEE, P. & RIAHI, D. N. 2005 On the development and validation of a numerical method for flows in thermal magnetic fluids and fields. In preparation.

BASSANO, E 2003 Numerical simulation of thermo-solutal-capillary migration of a dissolving drop in a cavity. International Journal of Numerical Methods in Fluids 41 (7), 765-788.

BOURDE, G. I. & SIMANOVSKII, I. B. 1979 Determination of equilibrium boundaries of a two-layered convection instability. J. Applied Math and Mech. 43, 1091-1097.

BRACKBILL JU, KOTHE DB, ZEMACH C., 1992 A continuum method for modeling surface tension. Journal of Computational Physics 100 (2), 335-354.

DAVIDSON MR, RUDMAN M. 2002 Volume-of-fluid calculation of heat or mass transfer across deforming interfaces in two-fluid flow Numerical Heat transfer Part B fundamentals S 41 (3-4), 291-308.

DAVIS, S. H. 1987 Thermocapillary instability. Ann. Rev. Fluid Mech. 19, 403-435.

DOI, T. & KOSTER, J. N. 1993 Thermocapillary convection in a two immiscible liquid layers with free interface. Phys. Fluids A5, 1914-1927.

DRAZIN, P. G. & REID, W. H. 1981 Hydrodynamic Stability, Cambridge University Press, UK.

FLORYAN, J. M. & RASMUSSEN, H. 1989 Numerical methods for viscous flows with moving boundaries, Appl. Mech. Rev. 42, 323-341.

GEORIS, P., HENNENBERG, M., SIMANOVSKII, I. B., NEPOMNYASHCHY, A. A., WERTGEIM, I. I. & LEGROS, J. C. 1993 Thermocapillary convection in a multilayer system. Phys. Fluids A5, 1575.

GEORIS, P., HENNENBERG, M., SIMANOVSKII, I. B., WERTGEIM, I. & LEGROS, J. C. 1994 Steady and oscillatory regimes of convective instability in multilayer systems. Microgravity Sci. & Techn. VII(2), 90.

GEORIS, P. & LEGROS, J. C. 1995 Pure thermocapillary convection in a multilayer system: first results from the IML-2 mission. Materials and Fluids Under Low Gravity, edited L. Ratke, H. Walter & B. Feuerbacher, New York: Springer, 299.

GEORIS, P., LEGROS, J. C., NEPOMNYASKCHY, A. A., SIMANOVSKII, I. B. & VIVIANI, A. 1997 Numerical simulation of convection flow in multilayer fluid systems. Microgravity Sci. Techn. X/1, 13.

GEORIS, P., HENNENBERG, M., LEBON, G. & LEGROS, J. C. 1999 Investigation of thermocapillary convection in a three-liquid-layer system. J. Fluid Mech. 389, 209.
GHIA K.N. and SHIN C.T. 1982 High-Re solutions for incompressible flow using the Navier-Stokes equations and a multi-grid method, - *J.Comp.Phys.*, v.48, 387-411.
GONDRET, P. & RABAUD, M. 1997 Shear instability of two-fluid parallel flow in a Hele-Shaw cell. Phys. Fluids 9, 3267-3274.
HAM, F. & YOUNG, Y. N. 2001 Numerical investigation of immiscible Rayleigh-Taylor problem using Cartesian adaptive grids. CFD Conference, Waterloo, Ontario.
HAMED, M. & FLORIAN, J. M. 2000 Marangoni convection. Part 1. A cavity with differentially heated sidewalls. J. Fluid Mech. 405, 79-110.
HJELLMING, L. N. & WALKER, J. S. 1987 Melt motion in a Czochralski crystal puller with an axial magnetic fielf: motion due to buoyancy and thermocapillarity. J. Fluid Mech. 182, 335-368.
HOU TY, LI ZL, OSHER S, *et al.* 1997 A hybrid method for moving interface problems with application to the Hele-Shaw flow JOURNAL OF COMPUTATIONAL PHYSICS 134 (2): 236-252.
HOYAS, S., HERRERO, H. & MANCHO, A. M. 2002 thermal convection in a cylindrical annulus heated laterally. J. Phys. A: Math. Gen. 35, 4067-4083.
IAFRATI, A., MASCIO, A. D. & CAMPANA, E. F. 2001 A level set technique applied to unsteady free surface. Int. J. Numer. Meth. Fluids 35, 281-297.
KATS-DEMIANETS, V., ORON, A. & NEPOMNYASHCHY, A. A. 1997a Linear stability of a tri-layer fluid system driven by the thermocaillary effect. Acta Astronaut 40, 655.
KATS-DEMIANETS, V., ORON, A. & NEPOMNYASHCHY, A. A. 1997b Marangoni instability and tri-layer liquid system. Eur. J. Mech. B/Fluids 16, 49.
KIM, Y. T., GOLDENFELD, N. & DANTZIG, J. 2000 Computation of dendritic microstructures using a level set method. Phys. Rev. E 62, 2471-2474.
KIMURA, T., HEYA, N., TAKEUCHI, M. & ISOMI, H. 1985 Natural convection in an enclosure with stratified fluids. Transactions of the Japanese Society of Mechanical Eng., 1251-1259.
KLIAKHANDLER, I. L., NEPOMNYASHCHY, A. A., SIMANOVSKII, I. B. & ZAKS, M. A. 1998 Nonlinear Marangoni waves in multilayer systems. Phys. Rev. E 58, 5765-5775.
KLIAKHANDLER, I. L. & NEPOMNYASHCHY, A. A. 1999 Kinetic instabilities of three-layer thermocapillary creeping flows. Phys. Fluids 11, 2139-2142.
KNIGHT, R. W. & PALMER, M. E. 1983 Simulation of free convection in multiple fluid layers in an enclosure by finite difference. Numerical Properties and Methodologies in Heat Transfer, edited by T. M. Shih, hemisphere, Washington, DC, 305-319.
LESLIE, F. W. & RAMACHANDRAN, N. 2001 A technique for rapidly deploying a concentration gradient with applications to microgravity. Exp. In Fluids 30, 568-577.
LI ZL., A fast iterative algorithm for elliptic interface problems Siam Journal on Numerical Analysis 35 (1): 230-254 FEB 1998
LIE, K. H., RIAHI, D. N. & WALKER, J. S. 1989 Buoyancy and surface tension driven flows in float zone crystal growth with a strong axial magnetic field. Int. J. Heat Mass Transfer 32, 2409-2420.
LIE, K. H., WALKER, J. S. & RIAHI, D. N. 1991 Melt motion in the float zone process with an axial magnetic field. J. Crystal Growth 109, 167-173.

LIU, Q. S. & ROUX, B. 1992 Instability of thermocapillary convection in multiple superimposed immiscible liquid layers.Proceedings of the VIII European Symposium on Materials and Fluid Sciences in Microgravity, European Space agency, S-333, Paris, 735.
LORSTAD D, FRANCOIS M, SHYY W, *et al.* 2004 Assessment of volume of fluid and immersed boundary methods for droplet computations International Journal for Numerical Methods in Fluids 46 (2): 109-125.
MCCLOUD, K. V. & MAHER, J. V. 1995 Experimental perturbations to Saffman-Taylor flow, Physics Reports 260, 139-185.
MIRANDA, J. A. & WIDOM, M. 2000 Parallel flow in Hele-Shaw cells with ferrofluids. Phys. Rev. E 61, 2114-2117.
MONTI, R. 2001 Physics of Fluids in Microgravity, Taylor & Francis, London and New York.
MORTHLAND, T. E. & WALKER, J. S. 1996 Thermocapillary convection during floating-zone silicon growth with a uniform or non-uniform magnetic field. J. Crystal Growth 158, 471-479.
MORTHLAND, T. E. & WALKER, J. S. 1997a Convective heat transfer due to thermocapillary convection with a strong magnetic field parallel to the free surface. Int. J. Heat Mass Transfer 40, 3283-3291.
MORTHLAND, T. E. & WALKER, J. S. 1997b Thermocapillary convection in a cylindrical liquid-metal floating zone with a strong azial magnetic field and with a non-axistmmetric heat flux. J. Fluid Mech. 345, 31-43.
MYRUM, T. A., SPARROW, E. M. & PRATA, A. T. 1986 Numerical solutions for natural convection in a complex enclosed space containing either air-liquid or liquid-liquid layers.Numerical Heat Transfer 10, 19-43.
NEPOMNYASHCHY, A. A. & SIMANOVSKII, I. B. 1990 Long wave thermocapillary convection in the layer with deformable interface. J. Appl. Math. Mech. 54,490.
NEPOMNYASHCHY, A. A. & SIMANOVSKII, I. B. 1997 New type of long wave oscillatory Marangoni instabilities. Quart. J. Mech. & Appl. Math. 50,149.
NEPOMNYASHCHY, A. A. & SIMANOVSKII, I. B. 1999 Combined action of different mechanisms of convective instability in multilayer systems. Phys. Rev. E 16, 6672.
NEURINGER, J. L. & ROSENSWEIG, R. E. 1964 Ferrohydrodynamics. Phys. Fluids 7, no. 12, 1927.
OSHER, S. & SETHIAN, J. A. 1988 Front propagating with curvature-dependent speed: algorithm based on Hamilton-Jacobi formulation. J. Computational Phys. 79, 12-49.
PEARSON, J. R. 1958., On convection cells induced by surface tension. J. Fluid Mech. 4, 489-500.
PRAKASH, A. & KOSTER, J. N. 1993 Natural and thermocapillary convection in three layers. Eur. J. Mech. B/Fluids 12, 635.
PRAKASH, A. & KOSTER, J. N. 1994a Convection in multilayers of immiscible liquids in shallow cavities, part I: Study natural convection. Int J. Multiphase Flow 20,383.
PRAKASH, A. & KOSTER, J. N. 1994b Convection in multilayers of immiscible liquids in shallow cavities, part II: Steady thermocapillary convection. Int. J. Multiphase Flow 20, 397.
PRAKASH, A. & KOSTER, J. N. 1994c Thermocapillary convection in three immiscible liquid layers. Microgravity Q4, 47.
RAMACHANDRAN, N. 1993 Thermal buoyancy and Marangoni convection in a two fluid layered system. J. Thermophysics and Heat Transfer 7, 352-360.
RAMACHANDRAN, N. & DOWNEY, J. P. 1994 Three-dimensional numerical investigation of gravitational and solutal effects in a cylindrical cell. J. Spacecraft and Rockets 31, 304-311.

RAMACHANDRAN, N. & LESLIE, F. W. 2001 Magnetic susceptibility effects and Lorentz force damping in diamagnetic fluids. AIAA-2001-0618,1-12.
RIAHI, D. N. 1993 Directional solidification of a binary alloy with deformed melt-crystal interface and hydromagnetic effects. Int. J. Eng. Sci. 30, 551-559.
RIAHI, D. N. 1994 Nonlinear Benard-Marangoni convection in a rotating layer. Lett. Appli. Eng. Sci. 32, 877-882.
RIAHI, D. N. 1996 Modal package convection in a horizontal porous layer with boundary imperfections. J. Fluid Mech. 318, 107-128.
RIAHI, D. N. 1999 Boundary layer theory of magneto-hydrodynamic turbulent convection.Proceedings of Indian National Science Academy (Physical Science) 65A, 109-116.
RIAHI, D. N. 2001 Effects of centrifugal and Coriolis forces on a hydromagnetic chimney convection in a mushy layer. J. Crystal Growth 226, 393-405.
RIAHI, D. N. 2002 Nonlinear convection in mushy layers. Part 1. Oscillatory modes of convection. J. Fluid Mech. 467, 331-359.
RIAHI, D. N. & WALKER, J. S.1989 Float zone shape and stability with the electromagnetic body force due to a radio-frequency induction coil. J. Crystal Growth 94, 635-642.
RIDER, W. J. & KOTHE, D. B. 1998 Reconstructing volume tracking. J. Comput. Physics 141, 112-152.
ROSENSWEIG, R. E. 1985 Ferrohydrodynamics. Cambridge University Press.
SAFFMAN, P. G. & TAYLOR, G. I. 1958 The penetration of a fluid into a porous medium or Hele-Shaw cell containing a more viscous fluid. Proc. Roy. Soc. A 245, 312-329.
SEN, A. K. & DAVIS, S. H. 1982 Steady thermocapillary flows in two-dimensional slots. J. Fluid Mech. 121, 163-186.
SHILOMIS, M. I. & RAIKHER, Y. L. 1980 Experimental investigations of magnetic fluids. IEEE Trans., Mag., MAG-16, 2, 237-250.
SIMANOVSKII, I. B. 1979 Numerical investigation of convection in a system of two immiscible fluids heated from below. Izvesnya Urali'skii Nauchanyi Tsentr, Akad. Nauk USSR, Sverdlovsk, USSR, 126-131.
SIMANOVSKII, I. B., GEORIS, P., HENNENBERG, M., VAN VAERENBERG, S., WERTGEIM, I. & LEGROS, J. C. 1992 Numerical investigation on Marangoni-Benard instability in multi layer systems.Proceedings of VIII European Symposium on Materials and Fluid sciences in Microgravity, European Space agency SP-333, Paris, 729.
SMEREKA, P. 2000 Spiral crystal growth. Physica D 138, 282-301.
SMITH, M. K. & DAVIS, S. H. 1983a Instabilities of dynamic thermocapillary liquid layers. Part 1. Convective instabilities. J. Fluid Mech.132, 119-144.
SMITH, M. K. & DAVIS, S. H. 1983b Instabilities of dynamic thermocapillary liquid layers. Part 2. Surface-wave instabilites. J. Fluid Mech. 132, 145-162.
SMITH, M. K., MIKSIS, M. J., MCFADDEN, G. B., NEITZEL, G. P. & CANRIGHT, D. R. 2002 Interface for the 21th Century, Imperial College Press.
SPARROW, E. M., AZEVEDO, L. F. A. & PRATA, A. T. 1986 Two-fluid and single-fluid natural convection heat transfer in an enclosure. J. heat Transfer 108, 848-852.
SUDO, S., HASHIMOTO, H. & IKEDA, A. 1989 Measurements of the surface tension of a magnetic fluid and interfacial phenomena. JSME Intl. Journal, II, 32, 1, 47-51.
SUSSMANN, M. P., SMEREKA, P. & OSHER, S. 1994 A level set approach for computing solutions to incompressible two-phase flow. J. Comput. Phys. 114, 146-159.

SZCKELY, J. & TODD, R. M. 1971 Natural convection in a rectangular cavity: Transient behavior and two-phase systems in laminar flow. J. Heat and Mass transfer 14, 467-482.
VELARDE, M. G. & NEPOMNYASHCHY, A. A. 2001 Interfactial patterns and waves. Physics of Fluids in Microgravity, edited by R. Monti, Taylor & Francis, London and NY, 126-148.
WHITHAM, G. B. 1974 Linear and Nonlinear Waves, New York: John Wiley & Sons.
XU, J. & ZEBIB, A. 1998 Oscillatory two- and three-dimensional thermocapillary convection. J. Fluid Mech. 364, 187-209.
YUE, W., LIN, C-L & PATEL, V. C. 2003 Numerical simulation of unsteady multidimensional free surface motions by level set method. Int. J. Numer. Meth. Fluids 42, 853-884.
ZAHN, M. 2001 Magnetic fluid and nanoparticle applications to nanotechnology. J. Nanoparticle Res. 3, 73-78.
ZEYBEK, M. & YORTSOS, Y. C. 1991 Long waves in parallel flow in Hele-Shaw cells. Phys. Rev. Lett. 67,1430-1433.
ZHONG, C. W. & WAKAYAMA, N. I. 2001 Effect of a high magnetic field on the viscosity of an aqueous solution of protein. J. Crystal Growth 226, 327-332.

List of Recent TAM Reports

No.	*Authors*	*Title*	*Date*
998	Christensen, K. T., and R. J. Adrian	The velocity and acceleration signatures of small-scale vortices in turbulent channel flow—*Journal of Turbulence*, in press (2002)	Jan. 2002
999	Riahi, D. N.	Flow instabilities in a horizontal dendrite layer rotating about an inclined axis—*Journal of Porous Media* **8**, 327–342 (2005)	Feb. 2002
1000	Kessler, M. R., and S. R. White	Cure kinetics of ring-opening metathesis polymerization of dicyclopentadiene—*Journal of Polymer Science A* **40**, 2373–2383 (2002)	Feb. 2002
1001	Dolbow, J. E., E. Fried, and A. Q. Shen	Point defects in nematic gels: The case for hedgehogs—*Archive for Rational Mechanics and Analysis* **177**, 21–51 (2005)	Feb. 2002
1002	Riahi, D. N.	Nonlinear steady convection in rotating mushy layers—*Journal of Fluid Mechanics* **485**, 279–306 (2003)	Mar. 2002
1003	Carlson, D. E., E. Fried, and S. Sellers	The totality of soft-states in a neo-classical nematic elastomer—*Journal of Elasticity* **69**, 169–180 (2003) with revised title	Mar. 2002
1004	Fried, E., and R. E. Todres	Normal-stress differences and the detection of disclinations in nematic elastomers—*Journal of Polymer Science B: Polymer Physics* **40**, 2098–2106 (2002)	June 2002
1005	Fried, E., and B. C. Roy	Gravity-induced segregation of cohesionless granular mixtures—*Lecture Notes in Mechanics*, in press (2002)	July 2002
1006	Tomkins, C. D., and R. J. Adrian	Spanwise structure and scale growth in turbulent boundary layers—*Journal of Fluid Mechanics* (submitted)	Aug. 2002
1007	Riahi, D. N.	On nonlinear convection in mushy layers: Part 2. Mixed oscillatory and stationary modes of convection—*Journal of Fluid Mechanics* **517**, 71–102 (2004)	Sept. 2002
1008	Aref, H., P. K. Newton, M. A. Stremler, T. Tokieda, and D. L. Vainchtein	Vortex crystals—*Advances in Applied Mathematics* **39**, in press (2002)	Oct. 2002
1009	Bagchi, P., and S. Balachandar	Effect of turbulence on the drag and lift of a particle—*Physics of Fluids*, in press (2003)	Oct. 2002
1010	Zhang, S., R. Panat, and K. J. Hsia	Influence of surface morphology on the adhesive strength of aluminum/epoxy interfaces—*Journal of Adhesion Science and Technology* **17**, 1685–1711 (2003)	Oct. 2002
1011	Carlson, D. E., E. Fried, and D. A. Tortorelli	On internal constraints in continuum mechanics—*Journal of Elasticity* **70**, 101–109 (2003)	Oct. 2002
1012	Boyland, P. L., M. A. Stremler, and H. Aref	Topological fluid mechanics of point vortex motions—*Physica D* **175**, 69–95 (2002)	Oct. 2002
1013	Bhattacharjee, P., and D. N. Riahi	Computational studies of the effect of rotation on convection during protein crystallization—*International Journal of Mathematical Sciences* **3**, 429–450 (2004)	Feb. 2003
1014	Brown, E. N., M. R. Kessler, N. R. Sottos, and S. R. White	*In situ* poly(urea-formaldehyde) microencapsulation of dicyclopentadiene—*Journal of Microencapsulation* (submitted)	Feb. 2003
1015	Brown, E. N., S. R. White, and N. R. Sottos	Microcapsule induced toughening in a self-healing polymer composite—*Journal of Materials Science* (submitted)	Feb. 2003
1016	Kuznetsov, I. R., and D. S. Stewart	Burning rate of energetic materials with thermal expansion—*Combustion and Flame* (submitted)	Mar. 2003
1017	Dolbow, J., E. Fried, and H. Ji	Chemically induced swelling of hydrogels—*Journal of the Mechanics and Physics of Solids*, in press (2003)	Mar. 2003
1018	Costello, G. A.	Mechanics of wire rope—Mordica Lecture, Interwire 2003, Wire Association International, Atlanta, Georgia, May 12, 2003	Mar. 2003
1019	Wang, J., N. R. Sottos, and R. L. Weaver	Thin film adhesion measurement by laser induced stress waves—*Journal of the Mechanics and Physics of Solids* (submitted)	Apr. 2003

No.	*Authors*	*Title*	*Date*
1020	Bhattacharjee, P., and D. N. Riahi	Effect of rotation on surface tension driven flow during protein crystallization—*Microgravity Science and Technology* **14**, 36–44 (2003)	Apr. 2003
1021	Fried, E.	The configurational and standard force balances are not always statements of a single law—*Proceedings of the Royal Society* (submitted)	Apr. 2003
1022	Panat, R. P., and K. J. Hsia	Experimental investigation of the bond coat rumpling instability under isothermal and cyclic thermal histories in thermal barrier systems—*Proceedings of the Royal Society of London A* **460**, 1957–1979 (2003)	May 2003
1023	Fried, E., and M. E. Gurtin	A unified treatment of evolving interfaces accounting for small deformations and atomic transport: grain-boundaries, phase transitions, epitaxy—*Advances in Applied Mechanics* **40**, 1–177 (2004)	May 2003
1024	Dong, F., D. N. Riahi, and A. T. Hsui	On similarity waves in compacting media—*Horizons in World Physics* **244**, 45–82 (2004)	May 2003
1025	Liu, M., and K. J. Hsia	Locking of electric field induced non-180° domain switching and phase transition in ferroelectric materials upon cyclic electric fatigue—*Applied Physics Letters* **83**, 3978–3980 (2003)	May 2003
1026	Liu, M., K. J. Hsia, and M. Sardela Jr.	In situ X-ray diffraction study of electric field induced domain switching and phase transition in PZT-5H—*Journal of the American Ceramics Society* (submitted)	May 2003
1027	Riahi, D. N.	On flow of binary alloys during crystal growth—*Recent Research Development in Crystal Growth* **3**, 49–59 (2003)	May 2003
1028	Riahi, D. N.	On fluid dynamics during crystallization—*Recent Research Development in Fluid Dynamics* **4**, 87–94 (2003)	July 2003
1029	Fried, E., V. Korchagin, and R. E. Todres	Biaxial disclinated states in nematic elastomers—*Journal of Chemical Physics* **119**, 13170–13179 (2003)	July 2003
1030	Sharp, K. V., and R. J. Adrian	Transition from laminar to turbulent flow in liquid filled microtubes—*Physics of Fluids* (submitted)	July 2003
1031	Yoon, H. S., D. F. Hill, S. Balachandar, R. J. Adrian, and M. Y. Ha	Reynolds number scaling of flow in a Rushton turbine stirred tank: Part I—Mean flow, circular jet and tip vortex scaling—*Chemical Engineering Science* (submitted)	Aug. 2003
1032	Raju, R., S. Balachandar, D. F. Hill, and R. J. Adrian	Reynolds number scaling of flow in a Rushton turbine stirred tank: Part II—Eigen-decomposition of fluctuation—*Chemical Engineering Science* (submitted)	Aug. 2003
1033	Hill, K. M., G. Gioia, and V. V. Tota	Structure and kinematics in dense free-surface granular flow—*Physical Review Letters* **91**, 064302 (2003)	Aug. 2003
1034	Fried, E., and S. Sellers	Free-energy density functions for nematic elastomers—*Journal of the Mechanics and Physics of Solids* **52**, 1671–1689 (2004)	Sept. 2003
1035	Kasimov, A. R., and D. S. Stewart	On the dynamics of self-sustained one-dimensional detonations: A numerical study in the shock-attached frame—*Physics of Fluids* (submitted)	Nov. 2003
1036	Fried, E., and B. C. Roy	Disclinations in a homogeneously deformed nematic elastomer—*Nature Materials* (submitted)	Nov. 2003
1037	Fried, E., and M. E. Gurtin	The unifying nature of the configurational force balance—*Mechanics of Material Forces* (P. Steinmann and G. A. Maugin, eds.), in press (2003)	Dec. 2003
1038	Panat, R., K. J. Hsia, and J. W. Oldham	Rumpling instability in thermal barrier systems under isothermal conditions in vacuum—*Philosophical Magazine*, in press (2004)	Dec. 2003
1039	Cermelli, P., E. Fried, and M. E. Gurtin	Sharp-interface nematic–isotropic phase transitions without flow—*Archive for Rational Mechanics and Analysis* **174**, 151–178 (2004)	Dec. 2003
1040	Yoo, S., and D. S. Stewart	A hybrid level-set method in two and three dimensions for modeling detonation and combustion problems in complex geometries—*Combustion Theory and Modeling* (submitted)	Feb. 2004

List of Recent TAM Reports (cont'd)

No.	*Authors*	*Title*	*Date*
1041	Dienberg, C. E., S. E. Ott-Monsivais, J. L. Ranchero, A. A. Rzeszutko, and C. L. Winter	Proceedings of the Fifth Annual Research Conference in Mechanics (April 2003), TAM Department, UIUC (E. N. Brown, ed.)	Feb. 2004
1042	Kasimov, A. R., and D. S. Stewart	Asymptotic theory of ignition and failure of self-sustained detonations—*Journal of Fluid Mechanics* (submitted)	Feb. 2004
1043	Kasimov, A. R., and D. S. Stewart	Theory of direct initiation of gaseous detonations and comparison with experiment—*Proceedings of the Combustion Institute* (submitted)	Mar. 2004
1044	Panat, R., K. J. Hsia, and D. G. Cahill	Evolution of surface waviness in thin films via volume and surface diffusion—*Journal of Applied Physics* (submitted)	Mar. 2004
1045	Riahi, D. N.	Steady and oscillatory flow in a mushy layer—*Current Topics in Crystal Growth Research*, in press (2004)	Mar. 2004
1046	Riahi, D. N.	Modeling flows in protein crystal growth—*Current Topics in Crystal Growth Research*, in press (2004)	Mar. 2004
1047	Bagchi, P., and S. Balachandar	Response of the wake of an isolated particle to isotropic turbulent cross-flow—*Journal of Fluid Mechanics* (submitted)	Mar. 2004
1048	Brown, E. N., S. R. White, and N. R. Sottos	Fatigue crack propagation in microcapsule toughened epoxy—*Journal of Materials Science* (submitted)	Apr. 2004
1049	Zeng, L., S. Balachandar, and P. Fischer	Wall-induced forces on a rigid sphere at finite Reynolds number—*Journal of Fluid Mechanics* (submitted)	May 2004
1050	Dolbow, J., E. Fried, and H. Ji	A numerical strategy for investigating the kinetic response of stimulus-responsive hydrogels—*Computer Methods in Applied Mechanics and Engineering* **194**, 4447–4480 (2005)	June 2004
1051	Riahi, D. N.	Effect of permeability on steady flow in a dendrite layer—*Journal of Porous Media*, in press (2004)	July 2004
1052	Cermelli, P., E. Fried, and M. E. Gurtin	Transport relations for surface integrals arising in the formulation of balance laws for evolving fluid interfaces—*Journal of Fluid Mechanics* (submitted)	Sept. 2004
1053	Stewart, D. S., and A. R. Kasimov	Theory of detonation with an embedded sonic locus—*SIAM Journal on Applied Mathematics* (submitted)	Oct. 2004
1054	Stewart, D. S., K. C. Tang, S. Yoo, M. Q. Brewster, and I. R. Kuznetsov	Multi-scale modeling of solid rocket motors: Time integration methods from computational aerodynamics applied to stable quasi-steady motor burning—*Proceedings of the 43rd AIAA Aerospace Sciences Meeting and Exhibit* (January 2005), Paper AIAA-2005-0357 (2005)	Oct. 2004
1055	Ji, H., H. Mourad, E. Fried, and J. Dolbow	Kinetics of thermally induced swelling of hydrogels—*International Journal of Solids and Structures* (submitted)	Dec. 2004
1056	Fulton, J. M., S. Hussain, J. H. Lai, M. E. Ly, S. A. McGough, G. M. Miller, R. Oats, L. A. Shipton, P. K. Shreeman, D. S. Widrevitz, and E. A. Zimmermann	Final reports: Mechanics of complex materials, Summer 2004 (K. M. Hill and J. W. Phillips, eds.)	Dec. 2004
1057	Hill, K. M., G. Gioia, and D. R. Amaravadi	Radial segregation patterns in rotating granular mixtures: Waviness selection—*Physical Review Letters* **93**, 224301 (2004)	Dec. 2004
1058	Riahi, D. N.	Nonlinear oscillatory convection in rotating mushy layers—*Journal of Fluid Mechanics*, in press (2005)	Dec. 2004
1059	Okhuysen, B. S., and D. N. Riahi	On buoyant convection in binary solidification—*Journal of Fluid Mechanics* (submitted)	Jan. 2005

List of Recent TAM Reports (cont'd)

No.	Authors	Title	Date
1060	Brown, E. N., S. R. White, and N. R. Sottos	Retardation and repair of fatigue cracks in a microcapsule toughened epoxy composite—Part I: Manual infiltration—*Composites Science and Technology* (submitted)	Jan. 2005
1061	Brown, E. N., S. R. White, and N. R. Sottos	Retardation and repair of fatigue cracks in a microcapsule toughened epoxy composite—Part II: *In situ* self-healing—*Composites Science and Technology* (submitted)	Jan. 2005
1062	Berfield, T. A., R. J. Ong, D. A. Payne, and N. R. Sottos	Residual stress effects on piezoelectric response of sol-gel derived PZT thin films—*Journal of Applied Physics* (submitted)	Apr. 2005
1063	Anderson, D. M., P. Cermelli, E. Fried, M. E. Gurtin, and G. B. McFadden	General dynamical sharp-interface conditions for phase transformations in viscous heat-conducting fluids—*Journal of Fluid Mechanics* (submitted)	Apr. 2005
1064	Fried, E., and M. E. Gurtin	Second-gradient fluids: A theory for incompressible flows at small length scales—*Journal of Fluid Mechanics* (submitted)	Apr. 2005
1065	Gioia, G., and F. A. Bombardelli	Localized turbulent flows on scouring granular beds—*Physical Review Letters*, in press (2005)	May 2005
1066	Fried, E., and S. Sellers	Orientational order and finite strain in nematic elastomers—*Journal of Chemical Physics* **123**, 044901 (2005)	May 2005
1067	Chen, Y.-C., and E. Fried	Uniaxial nematic elastomers: Constitutive framework and a simple application—*Proceedings of the Royal Society of London A*, in press (2005)	June 2005
1068	Fried, E., and S. Sellers	Incompatible strains associated with defects in nematic elastomers—*Journal of Chemical Physics*, in press (2005)	Aug. 2005
1069	Gioia, G., and X. Dai	Surface stress and reversing size effect in the initial yielding of ultrathin films—*Journal of Applied Mechanics*, in press (2005)	Aug. 2005
1070	Gioia, G., and P. Chakraborty	Turbulent friction in rough pipes and the energy spectrum of the phenomenological theory—*arXiv:physics* 0507066 v1 8 Jul 2005	Aug. 2005
1071	Keller, M. W., and N. R. Sottos	Mechanical properties of capsules used in a self-healing polymer—*Experimental Mechanics* (submitted)	Sept. 2005
1072	Chakraborty, P., G. Gioia, and S. Kieffer	Volcán Reventador's unusual umbrella	Sept. 2005
1073	Fried, E., and S. Sellers	Soft elasticity is not necessary for striping in nematic elastomers—*Nature Physics* (submitted)	Sept. 2005
1074	Fried, E., M. E. Gurtin, and Amy Q. Shen	Theory for solvent, momentum, and energy transfer between a surfactant solution and a vapor atmosphere—*Physical Review E* (submitted)	Sept. 2005
1075	Chen, X., and E. Fried	Rayleigh–Taylor problem for a liquid–liquid phase interface—*Journal of Fluid Mechanics* (submitted)	Oct. 2005
1076	Riahi, D. N.	Mathematical modeling of wind forces—In *The Euler Volume* (Abington, UK: Taylor and Francis), in press (2005)	Oct. 2005
1077	Fried, E., and R. E. Todres	Mind the gap: The shape of the free surface of a rubber-like material in the proximity to a rigid contactor—*Journal of Elasticity*, in press (2006)	Oct. 2005
1078	Riahi, D. N.	Nonlinear compositional convection in mushy layers—*Journal of Fluid Mechanics* (submitted)	Dec. 2005
1079	Bhattacharjee, P., and D. N. Riahi	Mathematical modeling of flow control using magnetic fluid and field—In *The Euler Volume* (Abington, UK: Taylor and Francis), in press (2005)	Dec. 2005
1080	Bhattacharjee, P., and D. N. Riahi	A hybrid level set/VOF method for the simulation of thermal magnetic fluids—*International Journal of Numerical Methods in Engineering* (submitted)	Dec. 2005
1081	Bhattacharjee, P., and D. N. Riahi	Numerical study of surface tension driven convection in thermal magnetic fluids—*Journal of Crystal Growth* (submitted)	Dec. 2005